

Title	A model relating transpiration for Japanese cedar and cypress plantations with stand structure
Author(s)	Komatsu, Hikaru; Shinohara, Yoshinori; Kumagai, Tomo ' omi; Kume, Tomonori; Tsuruta, Kenji; Xiang, Yang; Ichihashi, Ryuji; Tateishi, Makiko; Shimizu, Takanori; Miyazawa, Yoshiyuki; Nogata, Mari; Laplace, Sophie; Han, Tseng; Chiu, Chen-Wei; Ogura, Akira; Saito, Takami; Otsuki, Kyoichi
Citation	Forest Ecology and Management (2014), 334: 301-312
Issue Date	2014-12-15
URL	<a href="http://hdl.handle.net/2433/191207">http://hdl.handle.net/2433/191207</a>
Right	© 2014 Elsevier B.V.
Type	Journal Article
Textversion	author

1 Title

2 A model relating transpiration for Japanese cedar and cypress plantations with stand  
3 structure

4

5 The name and the affiliation of the authors

6 Hikaru Komatsu<sup>1,2 \*</sup>, Yoshinori Shinohara<sup>3</sup>, Tomo'omi Kumagai<sup>4</sup>, Tomonori Kume<sup>5</sup>,  
7 Kenji Tsuruta<sup>2</sup>, Yang Xiang<sup>6</sup>, Ryuji Ichihashi<sup>6</sup>, Makiko Tateishi<sup>6</sup>, Takanori Shimizu<sup>7</sup>,  
8 Yoshiyuki Miyazawa<sup>8</sup>, Mari Nogata<sup>6</sup>, Sophie Laplace<sup>5</sup>, Tseng Han<sup>5</sup>, Chen-Wei Chiu<sup>6</sup>,  
9 Akira Ogura<sup>9</sup>, Takami Saito<sup>4</sup>, Kyoichi Otsuki<sup>6</sup>

10

11 <sup>1</sup> The Hakubi Center for Advanced Research, Kyoto University, Kyoto 606–8302, Japan

12 <sup>2</sup> Graduate School of Agriculture, Kyoto University, Kyoto 606-8502, Japan

13 <sup>3</sup> Faculty of Agriculture, Kyushu University, Fukuoka 812-8581, Japan

14 <sup>4</sup> Hydrospheric Atmospheric Research Center, Nagoya University, Chikusa-ku, Nagoya  
15 464-8601, Japan

16 <sup>5</sup> School of Forestry and Resource Conservation, National Taiwan University, Taipei 106,  
17 Taiwan

18 <sup>6</sup> Kasuya Research Forest, Kyushu University, Fukuoka 811-2415, Japan

19 <sup>7</sup> Forestry and Forest Products Research Institute, Matsunosato, Tsukuba, Ibaraki 305-  
20 8687, Japan

21 <sup>8</sup> Research Institute for East Asia Environments, Kyushu University, Motooka, Fukuoka

22 811-0395, Japan

23 <sup>9</sup> Ishikawa-ken Forest Experimental Station, Ishikawa 920-2114, Japan

24 \* Corresponding author

25

26 Full address, E-mail, telephone, and fax numbers:

27 Hikaru Komatsu, The Hakubi Center for Advanced Research, Kyoto University, Kyoto

28 606-8302, Japan

29 Tel/Fax: +81-75-753-5100/5310

30 E-mail: [kmthkr@gmail.com](mailto:kmthkr@gmail.com)

31

32 Abstract

33 Previous studies have revealed that changes in forest structure due to management (e.g.,  
34 thinning, aging, and clearcutting) could affect the forest water balance. However, there  
35 are unexplained variability in changes in the annual water balance with changing structure  
36 among different sites. This is the case even when analyzing data for specific  
37 species/regions. For a more advanced and process-based understanding of changes in the  
38 water balance with changing forest structure, we examined transpiration ( $E$ ) observed  
39 using the sap-flux method for 14 Japanese cedar and cypress plantations with various  
40 structure (e.g., stem density and diameter) in Japan and surrounding areas and developed  
41 a model relating  $E$  with structural parameters. We expressed  $E$  using the simplified  
42 Penman–Monteith equation and modeled canopy conductance ( $G_c$ ) as a product of  
43 reference  $G_c$  ( $G_{cref}$ ) when vapor pressure deficit is 1.0 kPa and functions expressing the  
44 responses of  $G_c$  to meteorological factors. We determined  $G_{cref}$  and parameters of the  
45 functions for the sites separately.  $E$  observed for the 14 sites was not reproduced well by  
46 the model when using mean values of  $G_{cref}$  and the parameters among the sites. However,  
47  $E$  observed for the sites was reproduced well when using  $G_{cref}$  determined for each site  
48 and mean values of the parameters of the functions among the sites, similar to the case  
49 when using  $G_{cref}$  and the parameters of the functions determined for each site. These  
50 results suggest that considering variations in  $G_{cref}$  among the sites was important to  
51 reproduce variations in  $E$ , but considering variations in the parameters of the functions

52 was not. Our analysis revealed that  $G_{cref}$  linearly related with the sapwood area on a stand  
53 scale ( $A$ ) and that  $A$  linearly related with stem density ( $N$ ) and powers of the mean stem  
54 diameter ( $d_m$ ). Thus, we proposed a model relating  $E$  with  $A$  (or  $N$  and  $d_m$ ), where  $G_{cref}$   
55 was calculated from  $A$  (or  $N$  and  $d_m$ ) and the parameters of the functions were assumed to  
56 be the mean values among the sites. This model estimates changes in  $E$  with changing  
57 structure from commonly available data ( $N$  and  $d_m$ ), and therefore helps improve our  
58 understanding of the underlying processes of the changes in the water balance for  
59 Japanese cedar and cypress plantations.

60

61 Key words: canopy conductance; forest structure; model; sapwood area; simplified  
62 Penman–Monteith equation; transpiration

63

64 1. Introduction

65 Changes in forest structure due to management (e.g., planting, growth, thinning,  
66 aging, and clearcutting) can affect the forest water balance. Numerous studies (Scott and  
67 Lesch, 1997; Cornish and Vertessy, 2001) have examined changes in the annual water  
68 balance with changing forest structure on the basis of catchment water balance data.  
69 Summarizing data derived from such studies and analyzing them using linear regression,  
70 researchers have identified several important parameters (e.g., the ratio of the cutting area  
71 to the total catchment area, annual rainfall, and leaf phenology) determining changes in  
72 annual runoff with changing structure (Bosch and Hewlett, 1982; Brown et al., 2005;  
73 Komatsu et al., 2011). However, there remains unexplained variability in changes in the  
74 annual water balance (Bosch and Hewlett, 1982; Brown et al., 2005). This is the case even  
75 for data for a single species within a specific region, although the variability is less  
76 pronounced (Adams and Fowler, 2006; Komatsu et al., 2011). This suggests the limitation  
77 of analyzing catchment water balance data simply using linear regression without  
78 considering underlying processes (e.g., canopy transpiration and interception  
79 evaporation). For a more advanced understanding of changes in the annual water balance  
80 with changing structure, examining relationships of canopy transpiration and interception  
81 for given species with various structure (e.g., stem density and diameter) would be useful  
82 (Komatsu et al., 2007d). Variations in stem density and diameter relate with the sapwood  
83 area on a stand scale and leaf area index, which could in turn relate with canopy

84 transpiration (Granier et al., 2000a; Ewers et al., 2011). Focusing on specific species  
85 would be useful in reducing factors to be considered, because there are factors (e.g., the  
86 clumping factor and stem conductivity) that could differ among different species and  
87 affect canopy transpiration (Baldocchi and Meyers, 1998; Zwieniecki and Holbrook,  
88 1998; Bréda, 2003).

89 Japanese cedar (*Cryptomeria japonica*) and cypress (*Chamaeryparis obtusa*) are  
90 major plantation species in Japan and surrounding areas such as China and Taiwan (Japan  
91 Forestry Agency, 2014). Examining the water balance of these plantations is highly  
92 important from a practical viewpoint. Forest management (e.g., thinning) has been  
93 performed to increase water resources in Japan, although its effectiveness has not been  
94 assessed sufficiently (Komatsu et al., 2010). Summarizing data for interception  
95 evaporation of Japanese cedar and cypress plantations (Hattori et al., 1982; Tanaka et al.,  
96 2005), Komatsu et al. (2007a) found a relationship between stem density and interception  
97 evaporation and then developed a model relating interception evaporation with stem  
98 density. However, there have been few studies examining the relationship between forest  
99 structure and canopy transpiration ( $E$ ) for Japanese cedar and cypress plantations.

100 To assess changes in the water balance of Japanese cedar and cypress plantations  
101 with changing forest structure, we developed a model relating  $E$  for Japanese cedar and  
102 cypress plantations with meteorological and structural variables. The model formulates  $E$   
103 using the simplified Penman–Monteith equation (McNaughton and Black, 1973; Jarvis

104 and McNaughton, 1986). Canopy conductance ( $G_c$ ) in the equation was written as a series  
105 of functions expressing responses of  $G_c$  to meteorological factors (Jarvis, 1976;  
106 Lohammer et al., 1980). This study comprises three steps. First, we calculated  $G_c$  using  
107  $E$  data derived employing the sap-flux method for 14 sites and the inverted form of the  
108 simplified Penman–Monteith equation to determine parameters of the model for the sites  
109 separately. Second, we assessed the importance of each parameter in determining  $E$  on  
110 the basis of sensitivity analysis. Third, we examined the relationship of the important  
111 parameters with structural parameters. Here, we tried to relate the structural parameters  
112 with commonly available data such as stem density and diameter for wide use of the  
113 model.

114         Models estimating  $E$  are roughly classified into two groups. One uses many  
115 empirical parameters for modeling stomatal/canopy conductance to avoid considering  
116 internal hydraulics and keep the model structure simple (Granier et al., 2000a; Komatsu,  
117 2004), while the other considers internal hydraulics (Domec et al., 2012; McDowell et al.,  
118 2013). Our model belongs to the former group. Most models of the former group focus  
119 on reproducing  $E$  for a specific site (Cienciala et al., 1994a,b; Granier and Bréda, 1996).  
120 Several models (Granier et al., 2000a; Komatsu, 2004) are applicable to various sites,  
121 similar to our model. Our model differs from these models in that our model focuses on  
122 two species, which suggests higher predictability of the model when applied to the species.  
123 Furthermore, our model differs from the models in that our model would be tested against



124  $E$  data recorded not only during growing seasons but during winter, suggesting higher  
125 reliability of the model to predict  $E$  on a long time scale (e.g., one year).

126

## 127 2. Theory

128 The model, using the simplified Penman–Monteith equation (McNaughton and  
129 Black, 1973; Jarvis and McNaughton, 1986), expresses  $E$  as

$$130 \quad E = \frac{\rho C_p G_c D}{\gamma \lambda}, \quad (1)$$

131 where  $\rho$  is the air density,  $C_p$  is the specific heat of air,  $G_c$  is canopy conductance,  $D$  is  
132 the vapor pressure deficit,  $\gamma$  is the psychrometric constant, and  $\lambda$  is the latent heat of water  
133 vaporization. This equation is derived from the Penman–Monteith equation under the  
134 assumption of complete coupling between the canopy and atmosphere.

135  $G_c$  is formulated as a product of the reference value of  $G_c$  when  $D$  is 1.0 kPa  
136 ( $G_{cref}$ , Oren et al., 1999) and functions expressing responses of  $G_c$  to meteorological  
137 factors (Jarvis, 1976; Lohammer et al., 1980):

$$138 \quad G_c = G_{cref} \cdot f(D) \cdot g(R) \cdot h(T), \quad (2)$$

139 where  $f(D)$ ,  $g(R)$ , and  $h(T)$  are functions expressing the responses of  $G_c$  to mean daytime  
140  $D$ , solar radiation ( $R$ ), and air temperature ( $T$ ), respectively.  $f(D)$ ,  $g(R)$ , and  $h(T)$  are  
141 respectively modeled as (Oren et al., 1999; Granier et al., 2000b)

$$142 \quad f(D) = 1.00 - \beta \cdot \ln(D), \quad (3)$$

$$143 \quad g(R) = \min \left\{ \left( \frac{R}{600} \right)^\delta, 1.00 \right\}, \quad (4)$$

$$144 \quad h(T) = \begin{cases} 1.00 & (T \geq \epsilon) \\ \frac{T-\zeta}{\epsilon-\zeta} & (\zeta < T < \epsilon) , \\ 0.00 & (T \leq \zeta) \end{cases} \quad (5)$$

145 where  $\beta$ ,  $\delta$ ,  $\epsilon$ , and  $\zeta$  are parameters. The model does not consider the effect of the soil  
 146 water deficit on  $G_c$ . Most previous studies, making continuous measurements of  $E$  (or its  
 147 substitutes) for forests in Japan including Japanese cedar and cypress plantations  
 148 (Komatsu et al., 2006; Kosugi et al., 2007; Kumagai et al., 2007), did not report a clear  
 149 reduction in  $G_c$  or  $E$  with a soil water deficit, although there were a few exceptions  
 150 (Tanaka et al., 2002; Komatsu et al., 2007c).

151 We hypothesized that considering the variation in  $G_{cref}$  among sites would be  
 152 important but considering variations in  $\beta$ ,  $\delta$ ,  $\epsilon$ , and  $\zeta$  among sites would not be in  
 153 reproducing  $E$  for the sites. Our hypothesis was based on results of previous studies.  $G_{cref}$   
 154 linearly relates with  $E$  in the simplified Penman–Monteith equation.  $G_{cref}$  values reported  
 155 previously (Granier et al., 2000a; Komatsu et al., 2012, 2013) often differ greatly among  
 156 different forest sites comprising the same species, implying that considering the variation  
 157 in  $G_{cref}$  among the sites is important in estimating  $E$ . Oren et al. (1999) and succeeding  
 158 studies (Addington et al., 2004; Ewers et al., 2008) noted a fairly conservative  $\beta$  among  
 159 different sites. Thus, assuming  $\beta$  as constant among sites might not introduce large errors  
 160 in  $E$  estimates. Komatsu et al. (2006) analyzed sap flux data on an hourly time scale for  
 161 a Japanese cedar plantation and pointed out that the control of  $G_c$  by  $R$  was important only

162 early in the morning and late afternoon, when  $E$  is small. This implies that assuming  $\delta$  as  
163 constant among sites would not introduce large errors in estimating  $E$  on a daily time  
164 scale.  $\varepsilon$  and  $\zeta$  affect  $E$  during winter, which accounts for a small portion of annual  $E$  for  
165 Japanese cedar and cypress plantations (Suzuki, 1980; Kumagai et al., 2014). Thus,  
166 assuming  $\varepsilon$  and  $\zeta$  as constant among sites might not introduce large errors in estimating  
167  $E$  on a longer time scale, such as one year.

168         We further hypothesized that  $G_{cref}$  would relate with the sapwood area on a stand  
169 scale ( $A$ ) for the following reasons. Kumagai et al. (2007) examined  $E$  for two cedar forest  
170 sites located nearby but having different  $A$ . The relative difference in  $E$  between the sites  
171 was comparable to that in  $A$ . Komatsu et al. (2013) compared  $E$  values for a cedar forest  
172 during two successive growing seasons just before and after thinning. The ratio of  $E$  after  
173 thinning to that before thinning approximated the ratio of  $A$  after thinning to that before  
174 thinning. The results of Kumagai et al. (2007) and Komatsu et al. (2013) suggest a  
175 correlation between  $A$  and  $G_{cref}$ . Previous studies (Macfarlane et al., 2010; Ewers et al.,  
176 2011) reported relationships between  $A$  and  $E$  for forests comprising other species. These  
177 results also suggest that our hypothesis is reasonable. The relationship between  $A$  and  
178  $G_{cref}$  would allow the estimation of  $G_{cref}$  with the input of  $A$ , and then the estimation of  $E$   
179 by assuming typical values of  $\beta$ ,  $\delta$ ,  $\varepsilon$ , and  $\zeta$  and using the simplified Penman–Monteith  
180 equation.

181

182 3. Data used

183 We used  $E$  data recorded for nine Japanese cedar and five Japanese cypress  
184 plantations (Table 1). Twelve of the 14 sites were located in western Japan, but the IK and  
185 XT sites were located in eastern Japan and in Taiwan, respectively. Structural parameters  
186 differed among the sites. Stem density ( $N$ ) ranged between 600 and 1575 stems  $\text{ha}^{-1}$  for  
187 cedar and between 350 and 2100 stems  $\text{ha}^{-1}$  for cypress. The mean diameter at breast  
188 height ( $d_m$ ) ranged between 13.5 and 48.4 cm. The leaf area index ( $L$ ), estimated using  
189 optical methods (see the footnote #2 of Table 1), ranged between 0.8 and 5.9  $\text{m}^2 \text{m}^{-2}$  for  
190 cedar and between 0.8 and 4.8  $\text{m}^2 \text{m}^{-2}$  for cypress. Note that  $L$  for Japanese cedar and  
191 cypress forests estimated using optical methods is generally lower than that estimated  
192 using destructive leaf sampling and/or allometry equations (Hasegawa et al., 2013;  
193 Tsuruta et al., 2014). The sapwood area at a stand scale ( $A$ ) ranged between 14.1 and 46.0  
194  $\text{m}^2 \text{ha}^{-1}$  for cedar and between 8.8 and 20.4  $\text{m}^2 \text{m}^{-2}$  for cypress.  $A$  was determined by  
195 measurements of sapwood thickness using core sampling and assuming the stem cross-  
196 section was circular. A complete description of the measurements was provided by  
197 Kumagai et al. (2007) and Kume et al. (2010).

198  $E$  values for all sites were measured employing the sap-flux method and Granier  
199 sensors (Granier, 1987). A detailed description of the measurements is available in the  
200 papers cited in Table 1. Employing the method,  $E$  was estimated as (Kumagai et al., 2007;  
201 Kume et al., 2010)

202 
$$E = \frac{\sum_{i=1}^n F_i \cdot a_i}{S}, \quad (6)$$

203 where  $F$  is the sap flux for an individual tree averaged over its sapwood area,  $a$  is the tree  
204 sapwood area,  $n$  is the number of trees in the plot, and  $S$  is the ground area. For a tree  
205 whose sapwood thickness was much greater than the sensor length (i.e., 2.0 cm), two or  
206 three sensors were installed radially to cover the sapwood area (Kumagai et al., 2007).  $F$   
207 was calculated as the weighted average of sap flux for the sensors. Azimuthal variations  
208 of sap flux were also considered for some sites (Shinohara et al., 2013a).

209

#### 210 4. Methods of analysis

##### 211 4.1. Determination of parameters

212 We calculated canopy conductance ( $G_c$ ) from  $E$  estimated using the sap-flux  
213 method and meteorological factors for each site using the inverted form of the simplified  
214 Penman–Monteith equation:

215 
$$G_c = \frac{\gamma \lambda E}{\rho c_p D}. \quad (7)$$

216  $G_c$  was calculated as a daily average conductance using mean daytime  $T$  and  $D$ , and  $E$   
217 summed over 24 hr but divided by daylight hours (Phillips and Oren, 1998; Kumagai et  
218 al., 2008). Sap-flux sensors observe water movement through the trunk during nighttime,  
219 which may represent recharge of water into upper sections of the tree trunk and branches  
220 or transpiration during nighttime. Dividing  $E$  by daylight hours assumes that sap flux  
221 observed during nighttime represents recharge of water. Recent studies (Dawson et al.,

2007; Fisher et al., 2007; Oishi et al., 2008) have reported that transpiration during  
nighttime accounts for a considerable portion of daily transpiration. However,  
transpiration during nighttime would be very low in Japan possibly because of low  $D$   
during nighttime, as shown by measurements of transpiration using the leaf-chamber  
method (Kosugi et al., 1995, 1997; Tanaka et al., 2002). The “daytime” here was assumed  
as the period between 6 a.m. and 6 p.m. throughout the year for simplicity, i.e., the  
daylight hours were assumed as 12. These assumptions were also made in previous  
studies (Kumagai et al., 2008; Komatsu et al., 2012). We confirmed that these  
assumptions did not alter our conclusions.  $D$  for the period between 6 a.m. and 6 p.m.  
differed from  $D$  for the period between sunrise and sunset by no more than 8% for our  
sites. Our preliminary analysis revealed that  $G_c$  calculated using  $D$  for the period between  
6 a.m. and 6 p.m. could differ from those calculated using  $D$  for the period between sunset  
and sunrise by no more than 10%, which was not large enough to alter our conclusions.

We determined  $G_{cref}$ ,  $\beta$ , and  $\delta$  for the sites where  $E$  data only during the growing  
season were available. Here,  $h(T)$  was assumed to be 1.00 because of relatively high  $T$ .  
We determined  $G_{cref}$ ,  $\beta$ ,  $\delta$ ,  $\varepsilon$ , and  $\zeta$  for the sites where year-round  $E$  data were available.  
Note that analysis for the XT site did not follow this policy, as detailed later.

The parameters were determined in a manner similar to that employed by  
Komatsu et al. (2012, 2013). We first excluded data recorded on rainy days and days with  
 $D$  lower than 0.2 kPa. Data for sap flux (and therefore  $E$  and  $G_c$ ) could suffer from

242 measurement errors on rainy days (Kumagai et al., 2008; Komatsu et al., 2012).  $G_c$  could  
243 be highly affected by measurement errors in  $D$  when  $D$  is very low (Ewers and Oren,  
244 2000; Komatsu et al., 2007b). We then examined the relationship between  $D$  and  $G_c$  using  
245 data recorded on days with high  $R$  ( $>400 \text{ W m}^{-2}$ ) and  $T$  ( $>15 \text{ }^\circ\text{C}$ ). We determined  $G_{cref}$   
246 and  $\beta$  by regressing the relationship employing the least-squares method. After  
247 determining  $G_{cref}$  and  $\beta$ , we examined the relationship between  $R$  and observed  $G_c$  divided  
248 by  $G_{cref}f(D)$  using data recorded on days with high  $T$  ( $>15 \text{ }^\circ\text{C}$ ) to determine  $\delta$ . Here, we  
249 confirmed that the relationship between soil water content and observed  $G_c$  divided by  
250  $G_{cref}f(D)g(R)$  was generally unclear for sites where data for soil water content were  
251 available. We finally examined the relationship between  $T$  and observed  $G_c$  divided by  
252  $G_{cref}f(D)g(R)$  to determine  $\varepsilon$  and  $\zeta$ . Here, we also confirmed that the relationship between  
253  $T$  and observed  $G_c$  divided by  $G_{cref}f(D)g(R)$  was generally unclear for the sites where  $E$   
254 data only during the growing season were available.

255         We applied a different method to the determination of parameters for XT. XT  
256 was located in a mountainous region under a humid subtropical climate. If we had applied  
257 the same method as that applied to other sites, we would have only limited data with  
258 which to examine the relationship between  $D$  and  $G_c$  because of a large number of rainy  
259 days and days with low  $R$ . The method applied to XT was as follows. We first excluded  
260 data recorded on days with daily rainfall more than 5.0 mm and days with  $D$  lower than  
261 0.2 kPa. We then examined the relationship between  $D$  and  $G_c$  using data recorded on

262 days with  $R$  no less than  $300 \text{ W m}^{-2}$ . We determined  $G_{cref}$  and  $\beta$  by regressing the  
263 relationship employing the least-squares method. Here, we confirmed that there was no  
264 systematic difference in  $G_c$  between days without rain and days with rain no more than  
265 5.0 mm. After determining  $G_{cref}$  and  $\beta$ , we examined the relationship between  $R$  and  
266 observed  $G_c$  divided by  $G_{cref}f(D)$  to determine  $\delta$ . In the above analysis, we did not exclude  
267 data using a criterion about  $T$ , because the range of  $T$  was narrow for XT and a large  
268 portion of the data satisfied  $T$  being no less than  $15 \text{ }^\circ\text{C}$ . We did not determine the  
269 parameters in  $h(T)$ , because we did not find a clear relationship between  $T$  and observed  
270  $G_c$  divided by  $G_{cref}f(D)g(R)$  for XT.

271

#### 272 4.2. Assessing the importance of parameters

273 We hypothesized that considering the variation in  $G_{cref}$  among the sites would be  
274 important but considering variations in  $\beta$ ,  $\delta$ ,  $\varepsilon$ , and  $\zeta$  among the sites would not be in  
275 reproducing  $E$  for the 14 sites (detailed in the theory). To verify this hypothesis, we  
276 calculated  $E$  for days with no rain and  $T$  no less than  $15 \text{ }^\circ\text{C}$  (corresponding to a growing  
277 season) for the sites using three different parameterizations: (P1G) the mean values of  
278  $G_{cref}$ ,  $\beta$ , and  $\delta$  among the sites, (P2G)  $G_{cref}$  determined for each site and the mean values  
279 of  $\beta$  and  $\delta$  among the sites, and (P3G)  $G_{cref}$ ,  $\beta$ , and  $\delta$  determined for each site. To evaluate  
280 the reproducibility of  $E$  by P1G, P2G, and P3G, we examined the relationships of the  
281 mean  $E$  for the days calculated using P1G, P2G, and P3G respectively with the mean



282 observed  $E$ . If the difference in reproducibility between P1G and P2G was found to be  
283 important, considering the variation in  $G_{cref}$  among the sites would be important in  
284 calculating the mean  $E$  for a growing season. If the difference in reproducibility between  
285 P2G and P3G was found to be unimportant, considering variations in  $\beta$  and  $\delta$  would not  
286 be important.

287           Similarly, we calculated  $E$  for days with no rain for sites having data recorded in  
288 winter as well as those recorded in a growing season using three different  
289 parameterizations: (P1W) the mean values of  $G_{cref}$ ,  $\beta$ ,  $\delta$ ,  $\varepsilon$ , and  $\zeta$  among the sites, (P2W)  
290  $G_{cref}$  determined for each site and the mean values of  $\beta$ ,  $\delta$ ,  $\varepsilon$ , and  $\zeta$  among the sites, and  
291 (P3W)  $G_{cref}$ ,  $\beta$ ,  $\delta$ ,  $\varepsilon$ , and  $\zeta$  determined for each site. To evaluate the reproducibility of  $E$   
292 by P1W, P2W, and P3W, we examined the relationships of the mean  $E$  for the days  
293 calculated using P1W, P2W, and P3W respectively with the mean observed  $E$ . If the  
294 difference in reproducibility between P1W and P2W was found to be important,  
295 considering the variation in  $G_{cref}$  would be important in calculating the mean  $E$  for a period  
296 including a growing season and winter. If the difference in reproducibility between P2W  
297 and P3W was found to be unimportant, considering variations in  $\beta$ ,  $\delta$ ,  $\varepsilon$ , and  $\zeta$  among the  
298 sites would not be important.

299           When evaluating the model reproducibility, we primarily focused on the mean  $E$   
300 on a longer time scale, because our model was intended to be used to improve our  
301 understanding of the forest water balance on a long time scale (see Section 1). For

302 assessing the importance of the difference in reproducibility between different  
303 parameterizations, we did not examine whether there was a statistically significant  
304 difference between errors in  $E$  estimates using different parameterizations. What we need  
305 to know is not whether there is a statistical difference, but whether the magnitude of the  
306 difference is important in a practical context (Bakan, 1966; Thompson, 1996, 1998;  
307 Nuzzo, 2014). We thus examined whether errors in estimates of the mean  $E$  made using  
308 the  $G_c$  model were less than potential errors in observed  $E$ . Kumagai et al. (2007) and  
309 Kume et al. (2010) examined uncertainty in  $E$  estimates made using the sap-flux method  
310 for Japanese cedar and cypress plantations. Sampling data for sap flux on a sensor scale  
311 repeatedly using the Monte-Carlo technique, Kumagai et al. (2007) and Kume et al.  
312 (2010) revealed that the standard variation of  $E$  estimates was generally 10% or more of  
313 the mean  $E$ . When considering that 95% of data theoretically fall in the range of two  
314 standard deviations above and below the mean, potential errors in observed  $E$  would be  
315 less than 20% of the value in most cases. If errors in  $E$  estimates made using different  
316 parameterizations were more than 20% of observed  $E$ , we would regard the difference in  
317 reproducibility as important.

318           In addition, we examined whether errors in estimates of the mean  $E$  made using  
319 the  $G_c$  model were less than those in interception evaporation estimates made using the  
320 model developed by Komatsu et al. (2007a) or its revised form developed by Komatsu et  
321 al. (submitted), because our  $G_c$  model was intended to be used with the interception

322 evaporation model to assess the water balance for Japanese cedar and cypress plantations  
323 (Komatsu et al., submitted). The typical errors in interception evaporation estimates for  
324 the period with  $T$  no less than 15 °C and for a year would be 0.22 and 0.20 mm day<sup>-1</sup>,  
325 respectively (Appendix A).

326

#### 327 4.3. Relating important parameters with species and structures

328 We examined the relationship between  $A$  and  $G_{cref}$  to model  $G_{cref}$  using  $A$ . After  
329 confirming correlation between the two variables, we regressed the relationship to obtain  
330 a linear equation relating  $G_{cref}$  with  $A$ . The intercept of the equation was assumed to be  
331 zero. The slope of the equation was determined employing the least-squares method. To  
332 examine the stability of the correlation and the slope, we calculated 95% confidence  
333 intervals of these variables employing the bootstrapping method (Efron, 1979; Diaconis  
334 and Efron, 1983). These intervals were “bias-corrected, accelerated” percentile intervals  
335 calculated in the manner described by Efron (1987) and Fox (2008).

336 As data for  $A$  are not usually available for most Japanese cedar and cypress  
337 plantations, we tried to relate  $A$  with the mean diameter at breast height ( $d_m$ ) and stem  
338 density ( $N$ ) data in the following way. Tsuruta et al. (2011) summarized data for the  
339 sapwood area at a tree scale ( $a$ ) for 81 cedar trees from six sites and 109 cypress trees  
340 from nine sites and examined the relationships between diameter at breast height ( $d$ ) and  
341  $a$  for these species. They did not find clear differences in the relationship among sites.

342 They regressed the data to develop general equations for the relationships:  $a = a_{ref} \cdot d^k$ ,  
 343 where  $a$  and  $d$  were respectively in units of  $\text{cm}^2$  and  $\text{cm}$  and  $a_{ref}$  and  $k$  were parameters.  
 344  $a_{ref}$  was 1.40 and 1.96  $\text{cm}^2$  for cedar and cypress, respectively.  $k$  was 1.55 and 1.42 for  
 345 cedar and cypress, respectively. Approximating this equation by the tangential line at  $d$   
 346 being equal to  $d_m$ ,  $A$  was expressed as

$$347 \quad A = N \cdot a_{ref} \cdot d_m^k. \quad (8)$$

348 To examine the validity of this method of estimating  $A$  from  $N$  and  $d_m$ , we  
 349 investigated the relationship between  $A$  estimated employing this method and observed  
 350  $A$ . For this validation, we used  $A$  data for YB, YA, IS, KL, KU, KS, XT, and IH, and  
 351 another cypress site of Sun et al. (2014). Data for the other six sites (i.e., IK, IR, OL, OU,  
 352 SK, and HW) were not used, because  $a$  data for the sites were used by Tsuruta et al. (2011)  
 353 to develop the relationship between  $d$  and  $a$ .

354

## 355 5. Results

### 356 5.1. Determination of parameters

357 Figure 1 shows the relationships between  $D$  and  $G_c$ , between  $R$  and  $G_c$  divided  
 358 by  $G_{cref} f(D)$ , and between  $T$  and  $G_c$  divided by  $G_{cref} f(D) g(R)$ . Here, we show data only  
 359 for OL as an example. Regressing these relationships and relationships for the other sites,  
 360 parameters for the sites were determined as listed in Table 2. The maximum  $G_{cref}$  (9.77  
 361  $\text{mm s}^{-1}$  for IK) among the sites was more than five times the minimum  $G_{cref}$  (1.76  $\text{mm s}^{-1}$

362 <sup>1</sup> for IH). We observed variations in  $f(D)$ ,  $g(R)$ , and  $h(T)$  among sites (Figure 2).

363

## 364 5.2. Assessing the importance of parameters

365           Figure 3 shows the relationships of the mean  $E$  for days with no rain and  $T$  no  
366 less than 15 °C calculated using P1G, P2G, and P3G with observed  $E$ .  $E$  calculated using  
367 the model was not strongly correlated ( $r = 0.454$ ) with observed  $E$  for P1G, but was  
368 strongly correlated ( $r = 0.993$  and  $0.997$ , respectively) and fell along the 1:1 line for P2G  
369 and P3G. Errors for P1G were often greater than potential errors in observed  $E$  and  
370 interception evaporation estimates, but errors for P2G and P3G were not. Figure 4 shows  
371 the relationships of mean  $E$  for days with no rain calculated using P1W, P2W, and P3W  
372 with observed  $E$  for sites having data recorded in winter as well as those recorded in a  
373 growing season.  $E$  calculated using the model was not strongly correlated ( $r = 0.597$ ) with  
374 observed  $E$  for P1W, but was strongly correlated ( $r = 0.999$  and  $>0.999$ , respectively) and  
375 fell along the 1:1 line for P2W and P3W. Errors for P1W were often greater than potential  
376 errors in observed  $E$  and interception evaporation estimates, but errors for P2W and P3W  
377 were not. These results suggest that considering the variation in  $G_{cref}$  among the sites was  
378 important for reproducing the mean  $E$  on a long time scale, but considering variations in  
379  $\beta$ ,  $\delta$ ,  $\varepsilon$ , and  $\zeta$  was not.

380           Besides the mean  $E$  on a long time scale, we also examined model reproducibility  
381 of seasonal and day-to-day variations in  $E$  using data on a daily time scale for sites where

382 year-round data were available. Figure 5 shows time series of  $E$  calculated using P1W,  
383 P2W, and P3W and observed  $E$ . Here, we show data only for OU as an example. The  
384 slope of the regression line for the relationship between calculated and observed  $E$  often  
385 fell outside the range between 0.8 and 1.2 for P1W, where the range corresponded to the  
386 uncertainty in observed  $E$ . However, the slope always fell in the range for P2W and P3W  
387 (Table 3). The determination coefficients for P1W and P2W were often lower than that  
388 for P3W. However, the difference was relatively small. These results suggest that  
389 considering the variation in  $G_{cref}$  among the sites was important for reproducing seasonal  
390 and day-to-day variations in  $E$ , but considering variations in  $\beta$ ,  $\delta$ ,  $\varepsilon$ , and  $\zeta$  was not.

391

### 392 5.3. Relating important parameters with species and structures

393  $G_{cref}$  tended to increase with  $A$  (Figure 6). The correlation coefficient ( $r$ ) was  
394 0.698 and the 95% confidence interval was (0.446, 0.951), when pooling data for cedar  
395 and cypress. The correlation between  $A$  and  $G_{cref}$  was stronger than that between  $L$  and  
396  $G_{cref}$  ( $r = 0.479$ ). The regression line was determined as  $G_{cref} = 0.157 A$ , where  $A$  and  $G_{cref}$   
397 were in units of  $\text{m}^2 \text{ha}^{-1}$  and  $\text{m s}^{-1}$ , respectively. The 95% confidence interval of the slope  
398 was (0.127, 0.195). Data for both cedar and cypress were located along the regression  
399 line, suggesting no clear difference in  $G_{cref}$  for a given  $A$  between cedar and cypress. Thus,  
400 the regression equation could be used to predict  $G_{cref}$  from  $A$  for both cedar and cypress  
401 plantations and then to predict  $E$ . Figure 7 shows the normal probability plot (Fujii, 2005;

402 Peck and Devore, 2005) for differences between  $G_{cref}$  estimated using the regression  
403 equation and observed  $G_{cref}$ , where the normal score in the y-axis indicates the difference  
404 divided by the standard deviation of the difference for the 14 sites. Data for all sites except  
405 SK and IK were approximated by a line, indicating that most of these data followed a  
406 normal distribution. However, data for SK and IK were located far from the line,  
407 suggesting that observed  $G_{cref}$  for these sites was higher than expected from the regression  
408 equation and a normal distribution of the differences between estimated and observed  
409  $G_{cref}$ .

410 Figure 8 compares  $A$  estimated from  $N$  and  $d_m$  and observed  $A$ . Data were  
411 generally located around the 1:1 line. The mean relative error (i.e., the ratio of the  
412 difference between estimated and observed  $A$  to observed  $A$ ) was 26%. The magnitude of  
413 this error is discussed in Section 6.3.

414

## 415 6. Discussion

### 416 6.1. Roles of $f(D)$ , $g(R)$ , and $h(T)$

417 Our model succeeded in reproducing  $E$  observed for the 14 sites, suggesting  
418 validity of our hypothesis. Our model includes three functions, i.e.,  $f(D)$ ,  $g(R)$ , and  $h(T)$ .  
419 These functions influence on calculated  $E$  differently. Omitting  $f(D)$  from Eq. (2) (i.e.,  
420 assuming  $f(D)$  being 1.0) causes overestimation of  $E$  during May–August (Figure 9a),  
421 resulting in a relatively low determination coefficient ( $R^2 = 0.740$ ) for the relationship

422 between calculated and observed  $E$ . This suggests that considering reduction in  $G_c$  with  
423 increasing  $D$  is important in reproducing  $E$  when  $D$  is high.

424 Omitting  $g(R)$  causes overestimation of  $E$  during October–January when  $R$  is  
425 relatively low. Omitting  $h(T)$  causes overestimation of  $E$  during January–February when  
426  $T$  is relatively low. However, the determination coefficients for these cases ( $R^2 = 0.792$   
427 and  $0.798$ , respectively) are higher than that for the case of omitting  $f(D)$ . This suggests  
428 that effects of omitting  $g(R)$  and  $h(T)$  on reproducing  $E$  on a daily time scale are less  
429 important than that of omitting  $f(D)$ .

430

## 431 6.2. Variability in $G_{cref}$

432  $G_{cref}$  values for SK and IK were higher than expected from the regression  
433 equation (Figure 7). There are technical factors that potentially affect variations in  $G_{cref}$   
434 among sites. An insufficient number of sensors for sap flux measurements could result in  
435 large errors in  $E$  estimates. Shinohara et al. (2013a) compared errors in  $E$  estimates  
436 introduced by ignoring tree-to-tree variations, radial variations, and circumference  
437 variations in sap flux for a Japanese cedar plantation. They concluded that tree-to-tree  
438 variations in sap flux are the primary factor of errors in  $E$  estimates. Previous studies  
439 (Kumagai et al., 2005, 2007; Kume et al., 2010; Shinohara et al., 2013b) reported that  
440 errors in  $E$  estimates for Japanese cedar and cypress were serious when the number of  
441 trees in which sensors were installed was low, especially when there were less than



442 approximately 10. Note that this threshold number would be species specific, because  
443 different threshold numbers were reported for other species (Oren et al., 1998; Mackay et  
444 al., 2010). There were approximately 10 in which sensors were installed at each site (10  
445 for SK and 9 for IK). Furthermore,  $E$  for IK estimated from sap flux data derived for nine  
446 trees differed less than 5% from that estimated from sap flux data derived for all 18 trees  
447 according to intensive measurements performed during May 16–18 and June 1–4, 2010  
448 for the site. Thus, the numbers of sensors at these sites are not likely a main factor  
449 explaining the higher  $G_{cref}$ .

450         The use of the simplified Penman–Monteith equation could also be a factor  
451 causing higher  $G_{cref}$ . Aerodynamic conductance, which is assumed as infinite in the  
452 simplified Penman–Monteith equation, generally ranges between 70 and 400  $\text{mm s}^{-1}$  for  
453 coniferous forests including Japanese cedar and cypress plantations (Stewart and Thom,  
454 1973; Yamanoi and Ohtani, 1992; Loustau et al., 1996; Tanaka et al., 1996). When  
455 assuming aerodynamic conductance as 70  $\text{mm s}^{-1}$  and calculating  $G_{cref}$  using the original  
456 Penman–Monteith equation (see the methods used by Komatsu et al., 2012),  $G_{cref}$  values  
457 for SK and IK are determined as 3.53 and 6.22  $\text{mm s}^{-1}$ , respectively. These  $G_{cref}$  data are  
458 located close to the regression line in Figure 6, implying that the use of the simplified  
459 Penman–Monteith equation might be a potential factor explaining the higher  $G_{cref}$  for the  
460 sites. Unfortunately, there have been no data for aerodynamic conductance observed at  
461 these sites. However, data for wind speed for IK are available. The relationship between

462  $D$  and  $G_c$  differed only slightly according to wind speed, suggesting that low aerodynamic  
463 conductance would not be the primary factor causing low  $G_{c_{ref}}$  for IK. Data for wind speed  
464 for SK were unavailable.

465 Besides the factors discussed above, age might be another possible factor  
466 explaining high  $G_{c_{ref}}$  for SK, which is younger than the other sites (Table 1). There have  
467 been several studies reporting or suggesting changes in sap flux on a stand scale with age  
468 for mono-specific forests (Tsuruta et al., 2008; Forrester et al. 2010). We do not have data  
469 for other sites of similar age to SK. We thus recommend examining  $G_{c_{ref}}$  for young  
470 Japanese cedar and cypress plantations.

471

### 472 6.3. Errors in $A$ estimates

473 We observed a clear correlation between estimated and observed  $A$  (Figure 8).  
474 However, the error in  $A$  estimates was relatively large. The mean relative error in  $A$   
475 estimates (26%) was comparable to that in  $G_{c_{ref}}$  estimates obtained using the regression  
476 equation in Figure 5 (24%). Thus, it would be better to use observed  $A$  to calculate  $G_{c_{ref}}$ ,  
477 if observed  $A$  is available.

478 The error in  $A$  estimates would be primarily caused by errors in  $a$  estimates using  
479 Tsuruta et al.'s (2011) equation, and only secondarily caused by errors due to tangential  
480 approximation of the equation (Eq. (8)). The tangential approximation could cause  
481 underestimation of  $A$ , because  $a$  values calculated using the tangential line are no more

482 than those calculated using the original equation. In fact,  $A$  estimated employing the above  
483 method did not always underestimate observed  $A$  (Figure 8).

484

#### 485 6.4. Possible applications and implications

486 Our model would be useful as a research tool for hydrologists. There have been  
487 many studies (Dung et al., 2012; Kubota et al., 2013) examining changes in the annual  
488 water balance with changing structure of Japanese cedar and cypress plantations due to  
489 forest management. There are large variations in the change in the annual water balance  
490 among studies. Our model, accompanied with the interception evaporation model  
491 developed by Komatsu et al. (2007a), could be used by hydrologists to calculate changes  
492 in  $E$  and interception evaporation for catchments and improve our understanding of  
493 underlying processes of the variations. Our model and the interception model are also  
494 useful in estimating spatial variations in  $E$  and interception evaporation on a landscape  
495 scale, when these models are used with forest inventory data.

496 As described above, our model has great potential for application. This is  
497 because our model can be used only with the inputs of commonly available data for forest  
498 structure (i.e.,  $N$  and  $d_m$ ) and meteorology (see Appendix B). Our model is specific to  
499 Japanese cedar and cypress plantations. However, our model is important in that it  
500 demonstrates how to relate  $E$  with commonly available data. The concept of our model  
501 would be useful in developing similar models to estimate  $E$  for mono-specific forests

502 comprising other species.

503           On the other hand, the model needs to be tested further. The sites for cedar and  
504 cypress plantations (Table 1) were located mainly in western Japan, where temperature is  
505 intermediate or higher in the distribution areas of cedar and cypress (Japan Forestry  
506 Agency, 2013). We do not have enough  $E$  data for cedar and cypress plantations recorded  
507 in regions where temperature is lower, except data for IK. The response of  $G_c$  to  
508 temperature for stands in this region might be different from that observed in this study.  
509 We thus recommend testing the applicability of the model using data derived for sites  
510 located in this region. Furthermore, it is preferable to test the model applicability using  
511 data for sites with various age classes. Ages of the sites (Table 1) ranged between 19 and  
512 99 years, which almost covers the age range for most Japanese cedar and cypress  
513 plantations in Japan (Japan Forestry Agency, 2013). However, many of the sites fall in  
514 the range of 40–60 years. Thus, applicability of our model has been tested sufficiently for  
515 stands within this age class, but has not been fully tested outside the age class. A major  
516 portion of Japanese cedar and cypress plantations in Japan falls in this age class,  
517 suggesting the practical usefulness of the model. On the other hand, the portion of older  
518 stands is expected to increase, because forestry in Japan has stagnated and cedar and  
519 cypress plantations have not been actively harvested (Komatsu et al., 2010). Therefore,  
520 we recommend testing the applicability of the model to stands outside the age class.

521

522 Acknowledgements

523           We express our sincere thanks to members of Kyushu University Forest for their  
524 dedicated efforts in initiating the sites. We acknowledge Dr. Xinchao Sun (Graduate  
525 School of Life and Environmental Sciences, University of Tsukuba, Japan) for providing  
526 sapwood-area data for their site. Thanks are also due to two anonymous reviewers for  
527 providing critical comments. This research has been supported by a CREST project  
528 (Development of Innovative Technologies for Increasing Watershed Runoff and  
529 Improving River Environment by the Management Practice of Devastated Forest  
530 Plantation).

531

532 Appendix. A. Errors in interception evaporation estimates

533           The interception evaporation model developed by Komatsu et al. (2007a) and its  
534 revised form developed by Komatsu et al. (submitted) typically have an error of 4% of  
535 incident rainfall. The period with  $T$  no less than 15 °C is typically April–October in  
536 regions where Japanese cedar and cypress are distributed and incident rainfall during the  
537 period is typically 1200 mm (National Astronomical Observatory, 2013). Annual rainfall  
538 in the regions is typically 1800 mm. Thus, the typical error in interception evaporation  
539 estimates for the period with  $T$  no less than 15 °C would be 48 mm, which was equivalent  
540 to 0.22 mm day<sup>-1</sup>. The typical error for a year would be 72 mm, which was equivalent to  
541 0.20 mm day<sup>-1</sup>.

542

543 Appendix. B. Methods of preparing meteorological inputs

544 The model developed in this study requires daytime (6 a.m.–6 p.m.) mean solar  
545 radiation ( $R$ ), temperature ( $T$ ), and vapor pressure deficit ( $D$ ) as meteorological inputs.  $R$   
546 data are not always available throughout Japan (Shinohara et al., 2007). It is often the  
547 case that only daily maximum ( $T_x$ ) and minimum temperatures ( $T_n$ ) are available for  
548 historical data (The University of Tokyo Forests, 2014).

549 The former problem can be solved by substituting  $R$  for the target area by data  
550 for solar radiation recorded at a meteorological observatory in surrounding areas. Data  
551 for daily solar radiation are recorded at main meteorological observatories in Japan (Japan  
552 Meteorological Agency, 2014).  $R$  in units of  $\text{W m}^{-2}$  can be approximated by daily solar  
553 radiation in units of  $\text{MJ m}^{-2} \text{day}^{-1}$  multiplied by an index of 23.1, which converts the units.  
554  $E$  during January 1–December 31, 2008 calculated using the model with the input of  $R$ ,  
555  $T$ , and  $D$  observed at OL is 234 mm. Here,  $G_{cref}$  is assumed to be  $0.00322 \text{ m s}^{-1}$  on the  
556 basis of observed  $A$  and the relationship between  $A$  and  $G_{cref}$  (Figure 6).  $E$  values during  
557 the same period calculated with the input of solar radiation observed at meteorological  
558 observatories at Fukuoka, Saga, Oita, and Hiroshima are 238, 234, 237, and 240 mm,  
559 respectively. These meteorological observatories are located 15, 50, 110, 200 km from  
560 OL, respectively. All these values approximate the value calculated using  $R$  for OL.  
561 Qualitatively, the same results are available for other sites. Thus, accurate estimates of  $R$

562 are not important for estimating  $E$  using the model. This is attributed to  $E$  being  
563 insensitive to  $R$  when  $R$  is high (Figure 2b) and  $E$  on days with high  $R$  accounting for a  
564 relatively large portion of annual  $E$ .

565         The latter problem (i.e., only  $T_x$  and  $T_n$  are available) can be solved making the  
566 following assumptions. First, the diurnal trend in temperature is approximated using a  
567 sine function minimized at 6 a.m. and maximized at 2 p.m. A similar approximation has  
568 been commonly used to produce hourly temperature data from  $T_x$  and  $T_n$  (Campbell and  
569 Norman, 1998). Under this assumption,  $T$  (i.e., temperature during 6 a.m.–6 p.m.) is  
570 analytically written as  $T = (T_x + T_n)/2 + (T_x - T_n)/(3\pi)$ . Second, vapor pressure deficit at  
571 6 a.m. is zero and daytime vapor pressure deficit is caused by a temperature rise during  
572 the day. Note that the assumption of vapor pressure deficit being zero in the morning is  
573 generally valid except in arid and semi-arid regions (Running et al., 1987; Kimball et al.,  
574 1994).  $D$  (i.e., the mean vapor pressure deficit during 6 a.m.–6 p.m.) is thus approximated  
575 by  $D = e_s(T) - e_s(T_n)$ , where  $e_s$  is the saturation vapor pressure.  $E$  during January 1–  
576 December 31, 2008 calculated using the model with the input of  $R$ ,  $T$ , and  $D$  observed at  
577 OL is 234 mm.  $E$  during the same period calculated with the input of  $R$ ,  $T_x$  and  $T_n$  observed  
578 at OL is 225 mm, which approximates  $E$  calculated with the input of  $T$  and  $D$ .  
579 Qualitatively, the same results are available for other sites.

580 References

- 581 Adams, K.N., Fowler, A.M., 2006. Improving empirical relationships for predicting the  
582 effect of vegetation change on annual water yield. *J. Hydrol.* 321, 90–115.
- 583 Addington, R.N., Mitchell, R.J., Oren, R., Donovan, L.A., 2004. Stomatal sensitivity to  
584 vapor pressure deficit and its relationship to hydraulic conductance in *Pinus palustris*.  
585 *Tree Physiol.* 24, 561–569.
- 586 Bakan, D., 1966. The test of significance in psychological research. *Psychol. Bull.* 66,  
587 423–437.
- 588 Baldocchi, D., Meyers, T.P., 1998. On using eco-physiological, micrometeorological and  
589 biogeochemical theory to evaluate carbon dioxide, water vapor and trace gas fluxes  
590 over vegetation: a perspective. *Agric. For. Meteorol.* 90, 1–25.
- 591 Bosch, J.M., Hewlett, J.D., 1982. A review of catchment experiments to determine the  
592 effect of vegetation changes on water yield and evapotranspiration. *J. Hydrol.* 55, 3–  
593 23.
- 594 Bréda, N.J.J., 2003. Ground-based measurements of leaf area index: a review of methods,  
595 instruments and current controversies. *J. Exp. Bot.* 54, 2403–2417.
- 596 Brown, A., Zhang, L., McMahon, T.A., Western, A.W., Vertessy, R.A., 2005. A review of  
597 paired catchment studies for determining changes in water yield resulting from  
598 alterations in vegetation. *J. Hydrol.* 310, 28–61.
- 599 Campbell, G.S., Norman, J.M., 1998. *An Introduction to Environmental Biophysics.*



600 Springer-Verlag, New York.

601 Cienciala, E., Eckersten, H., Lindroth, A., Hallgren, J., 1994a. Simulated and measured  
602 water uptake by *Picea abies* under non-limiting soil water conditions. Agric. For.  
603 Meteorol. 71, 147–164.

604 Cienciala, E., Lindroth, A., Cermak, J., Hallgren, J., Kucera, J., 1994b. The effects of  
605 water availability on transpiration, water potential and growth of *Picea abies* during a  
606 growing season. J. Hydrol. 155, 57–71.

607 Cornish, P.M., Vertessy, R.A., 2001. Forest age-induced changes in evapotranspiration  
608 and water yield in a eucalypt forest. J. Hydrol. 242, 43–63.

609 Dawson, T.E., Burgess, S.S.O., Tu, K.P., Oliveira, R.S., Santiago, L.S., Fisher, J.B.,  
610 Simonin, K.A., Ambrose, A.R., 2007. Nighttime transpiration in woody plants from  
611 contrasting ecosystems Tree Physiol. 27, 561–575.

612 Diadonis, P., Efron, B., 1983. Computer-intensive methods in statistics. Sci. Am. 248,  
613 116–131.

614 Domec, J.C., Ogée, J., Noormets, A., Jouangy, J., Gavazzi, M., Treasure, E., Sun, G.,  
615 McNulty, S.G., King, J.S., 2012. Interactive effects of nocturnal transpiration and  
616 climate change on the root hydraulic redistribution and carbon and water budgets of  
617 southern United States pine plantations. Tree Physiol. 32, 707–723.

618 Dung, B.X., Gomi, T., Miyata, S., Sidle, R.C., Kosugi, K., Onda, Y., 2012. Runoff  
619 responses to forest thinning at plot and catchment scales in a headwater catchment

620 draining Japanese cypress forest. *J. Hydrol.* 444–445, 51–62.

621 Efron, B., 1979. Bootstrap methods: another look at the Jackknife. *Ann. Stat.* 7, 1–26.

622 Efron, B., 1987. Better bootstrap confidence intervals. *J. Amer. Statist. Assoc.* 82, 171–  
623 185.

624 Ewers, B.E., Oren, R., 2000. Analyses of assumptions and errors in the calculation of  
625 stomatal conductance from sap flux measurements. *Tree Physiol.* 20, 579–589.

626 Ewers, B.E., Mackay, D.S., Tang, J., Bolstad, P.V., Samanta, S., 2008. Intercomparison of  
627 sugar maple (*Acer saccharum* Marsh.) stand transpiration responses to environmental  
628 conditions from the Western Great Lakes Region of the United States. *Agric. For.*  
629 *Meteorol.* 148, 231–246.

630 Ewers, B.E., Bond-Lamberty, B., Machay, D.S., 2011. Consequences of stand age and  
631 species' functional trait changes on ecosystem water use of forests, in Meinzer, F.C.,  
632 Lachenbruch, B., Dawson, T.E. (Eds.), *Size- and Age-Related Changes in Tree*  
633 *Structure and Function*. Springer, Dordrecht, pp. 481–505.

634 Fisher, J.B., Baldocchi, D.D., Misson, L., Dawson, T.E., Goldstein, A.H., 2007. What the  
635 towers don't see at night: nocturnal sap flow in trees and shrubs at two AmeriFlux sites  
636 in California. *Tree Physiol.* 27, 597–610.

637 Forrester, D.I., Collopy, J.J., Morris, J.M., 2010. Transpiration along an age series of  
638 *Eucalyptus globulus* plantations in southeastern Australia. *Forest Ecol. Manage.* 259,  
639 1754–1760.

640 Fox, J., 2008. Applied Regression Analysis and Generalized Linear Models. Sage  
641 Publications, Thousand Oaks, Carfornia.

642 Franzer, G.W., Ganha, C.D., Lertzman, K.P., 1999. Gap Light Analyzer (GLA) Version  
643 2.0: Image software to Extract Canopy Structure and Gap Light Transmission Indices  
644 from True-colour Fisheye Photographs. Simon Franzer University, British Columbia,  
645 and the Institute of Ecosystem Studies, Millbrook, New York, pp. 1–36.

646 Fujii, H., 2005. Practical Methods of Data Analysis for Engineers. Tokyo-Kagaku-Dojin,  
647 Tokyo.

648 Granier, A., 1987. Evaluation of transpiration in a Douglas-fir stand by means of sap flow  
649 measurements. *Tree Physiol.* 3, 309–320.

650 Granier, A., Bréda, N., 1996. Modelling canopy conductance and stand transpiration of  
651 an oak forest from sap flow measurements. *Ann. Sci. For.* 53, 537–546.

652 Granier, A., Loustau, D., Bréda, N., 2000a. A generic model of forest canopy conductance  
653 dependent on climate, soil water availability and leaf area index. *Ann. For. Sci.* 57,  
654 755–765.

655 Granier, A., Biron, P., Lemoine, D., 2000b. Water balance, transpiration and canopy  
656 conductance in two beech stands. *Agric. For. Meteorol.* 100, 291–308.

657 Hasegawa, K., Omi, H., Hiruma, Y., Kumagai, S., Yamamoto, R., Izumi, T., Matsuyama,  
658 H., 2013. Estimation of leaf area index of *Cryptomeria japonica* using various  
659 methods : A case study of Aso District, Kumamoto Prefecture. *J. Geograph.* 122, 875–

660 891.

661 Hattori, S., Chikaarashi, H., Takeuchi, N., 1982. Measurement of the rainfall interception  
662 and its micrometeorological analysis in a Hinoki stand. Bull. FFPRI 318, 79–102.

663 Ichihashi, R., Komatsu, H., Kume, T., Onozawa, Y., Shinohara, Y., Tsuruta, K., Otsuki,  
664 K., Stand-scale transpiration of two Moso bamboo stands with different culm densities.  
665 Ecohydrol. In press.

666 Japan Forestry Agency, 2013. White Paper for Forest and Forestry. Japan Forestry Agency,  
667 Tokyo. (Available at: <http://www.rinya.maff.go.jp/j/kikaku/hakusyo/index.html>).

668 Japan Forestry Agency, 2014. Data for Japanese cedar and cypress plantations.  
669 [http://www.rinya.maff.go.jp/j/sin\\_riyou/kafun/data.html](http://www.rinya.maff.go.jp/j/sin_riyou/kafun/data.html).

670 Japan Meteorological Agency, 2014. Meteorological statistics.  
671 <http://www.jma.go.jp/jma/menu/report.html>.

672 Jarvis, P.G., 1976. The interpretation of the variations in leaf water potential and stomatal  
673 conductance found in canopies in the field. Phil. Trans. R. Soc. Lond. B 273, 593–610.

674 Jarvis, P.G., McNaughton, K.G., 1986. Stomatal control of transpiration: scaling up from  
675 leaf to region. Adv. Ecol. Res. 15, 1–49.

676 Kimball, J.S., Running, S.W., Nemani, R. 1994. An improved method for estimating  
677 surface humidity from daily minimum temperature. Agric. For. Meteorol. 85, 87–98.

678 Komatsu, H., 2004. A general method of parameterizing the big-leaf model to predict the  
679 dry-canopy evaporation rate of individual coniferous forest stands. Hydrol. Process.

680 18, 3019–3036.

681 Komatsu, H., Kang, Y., Kume, T., Yoshifuji, N., Hotta, N., 2006. Transpiration from a  
682 *Cryptomeria japonica* plantation, part 2: responses of canopy conductance to  
683 meteorological factors. *Hydrol. Process.* 20, 1321–1334.

684 Komatsu, H., Tanaka, N., Kume, T., 2007a. Do coniferous forests evaporate more water  
685 than broad-leaved forests in Japan? *J. Hydrol.* 336, 361–375.

686 Komatsu, H., Hotta, N., Kume, T., 2007b. What is the best way to represent surface  
687 conductance for a range of vegetated sites? *Hydrol. Process.* 21, 1142–1147.

688 Komatsu, H., Katayama, A., Hirose, S., Kume, A., Higashi, N., Ogawa, S., Otsuki, K.,  
689 2007c. Reduction in soil water availability and tree transpiration in a forest with  
690 pedestrian trampling. *Agric. Forest Meteorol.* 146, 107–114.

691 Komatsu, H., Kume, T., Otsuki, K., 2007d. Contemporary role of catchment water  
692 balance data for forest evapotranspiration research. *J. Jpn. For. Soc.* 89, 346–359.

693 Komatsu, H., Kume, T., Otsuki, K., 2010. Water resource management in Japan—forest  
694 management or dam reservoirs? *J. Environ. Manage.* 91, 814–823.

695 Komatsu, H., Kume, T., Otsuki, K., 2011. Increasing annual runoff—broadleaf or  
696 coniferous forests? *Hydrol. Process.* 25, 302–318.

697 Komatsu, H., Onozawa, Y., Kume, T., Tsuruta, K., Shinohara, Y., Otsuki, K., 2012.  
698 Canopy conductance for a Moso bamboo (*Phyllostachys pubescens*) forest in western  
699 Japan. *Agric. For. Meteorol.* 156, 111–120.

700 Komatsu, H., Shinohara, Y., Nogata, M., Tsuruta, K., Otsuki, K., 2013. Changes in canopy  
701 transpiration due to thinning of a *Cryptomeria japonica* plantation. *Hydrol. Res. Lett.*  
702 7, 60–65.

703 Komatsu, H., Shinohara, Y., Otsuki, K., Models to predict changes in annual runoff with  
704 thinning and clearcutting of Japanese cedar and cypress plantations in Japan.  
705 Submitted to *Hydrol. Process.*

706 Kosugi, Y., Kobashi, S., Shibata, S., 1995. Modeling stomatal conductance on leaves of  
707 several temperate evergreen broad-leaved trees. *J. Jap. Reveget. Tech.* 20, 158–167.

708 Kosugi, Y., Shibata, S., Matsui, K., Kobashi, S., 1997. Differences between deciduous  
709 and evergreen broad-leaved trees in the pattern of seasonal change of leaf-scale  
710 photosynthetic net assimilation rate and transpiration rate. *J. Jap. Reveget. Tech.* 22,  
711 205–215.

712 Kosugi, Y., Takanashi, S., Tanaka, H., Ohkubo, S., Tani, M., Yano, M., Katayama, T.,  
713 2007. Evapotranspiration over a Japanese cypress forest. I. Eddy covariance fluxes  
714 and surface conductance characteristics for 3 years. *J. Hydrol.* 337, 269– 283.

715 Kubota, T., Tsuboyama, Y., Nobuhiro, T., Sawano, S., 2013. Change of evapotranspiration  
716 due to stand thinning in the Hitachi Ohta Experimental Watershed. *J. Jpn. For. Soc.* 95,  
717 37–41.

718 Kumagai, T., Aoki, S., Nagasawa, H., Mabuchi, T., Kubota, K., Inoue, S., Utsumi, Y. and  
719 Otsuki, K., 2005. Effects of tree-to-tree and radial variations on sap flow estimates of

720 transpiration in Japanese cedar. *Agric. For. Meteorol.* 135, 110–116.

721 Kumagai, T., Aoki, S., Shimizu, T., Otsuki, K., 2007. Sap flow estimates of stand  
722 transpiration at two slope positions in a Japanese cedar forest watershed. *Tree Physiol.*  
723 27, 161–168.

724 Kumagai, T., Tateishi, M., Shimizu, T., Otsuki, K., 2008. Transpiration and canopy  
725 conductance at two slope positions in a Japanese cedar forest watershed. *Agric. For.*  
726 *Meteorol.* 148, 1444–1455.

727 Kumagai, T., Tateishi, M., Miyazawa, Y., Kobayashi, M., Yoshifuji, N., Komatsu, H.,  
728 Shimizu, T., 2014. Estimation of annual forest evapotranspiration from a coniferous  
729 plantation watershed in Japan (1): Water use components in Japanese cedar stands. *J.*  
730 *Hydrol.* 508, 66–76.

731 Kume, T., Tsuruta, K., Komatsu, H., Kumagai, T., Higashi, N., Shinohara, Y., Otsuki, K.,  
732 2010. Effects of sample size on sap flux-based stand-scale transpiration estimates *Tree*  
733 *Physiol.* 30, 129–138.

734 Kume, T., Tsuruta, K., Komatsu, H., Shinohara, Y., Katayama, A., Ide, J., Otsuki, K.,  
735 Differences in sap flux based stand transpiration between upper and lower slope  
736 positions in a Japanese cypress plantation watershed. Submitted to *J. Hydrol.*

737 Laplace 2013. Study on Transpiration in a Taiwanese Moso Bamboo Forest using Sap  
738 Flow Measurement. Master thesis, National Taiwan University.

739 Lohammer, T., Linder, S., Falk, O., 1980. FAST-simulation models of gaseous exchange

740 in Scots. Pine. *Ecol. Bull. (Stockholm)* 32, 505–523.

741 Loustau, D., Berbigier, P., Roumagnac, P., Arruda-Pacheco, C., David, J.S., Ferreira, M.I.,  
742 Pereira, J.S., Tavares, R., 1996. Transpiration of a 64-year-old maritime pine stand in  
743 Portugal. 1. Seasonal course of water flux through maritime pine. *Oecologia* 107, 33–  
744 42.

745 Macfarlane, C., Bond, C., White, D.A., Grigg, A.H., Ogdena, G.N., Silberstein, R., 2010.  
746 Transpiration and hydraulic traits of old and regrowth eucalypt forest in southwestern  
747 Australia. *Forest Ecol. Manage.* 260, 96–105.

748 Mackay, D.S., Ewers, B.E., Loranty, M.M., Kruger, E.L., 2010. On the representativeness  
749 of plot size and location for scaling transpiration from trees to a stand. *J. Geophys.*  
750 *Res.* 115, G02016.

751 McDowell, N.G., Fisher, R.A., Xu, C., Domec, J.C., Hölttä, T., Mackay, D.S., Sperry, J.S.,  
752 Boutz, A., Dickman, L., Gehres, N., Limousin, J.M., Macalady, A., Martínez-Vilata,  
753 J., Mencuccini, M., Plaut, J.A., Ogée, J., Pangle, R.E., Rasse, D.P., Ryan, M.G.,  
754 Sevanto, S., Waring, R.H., Williams, A.P., Yopez, E.A., Pockman, W.T., 2013.  
755 Evaluating theories of drought-induced vegetation mortality using a multimodel–  
756 experiment framework. *New Phytol.* 200, 304–321.

757 McNaughton, K.G., Black, T.A., 1973. A study of evapotranspiration from a Douglas fir  
758 forest using the energy balance approach. *Water Resour. Res.* 9, 1579–1590.

759 National Astronomical Observatory, 2013. *Chronological Scientific Tables* 2014.



760 Maruzen, Tokyo.

761 Nuzzo, R., 2014. Statistical errors. *Nature* 506, 150–152.

762 Oishi, A.C., Oren, R., Stoy, P.C., 2008. Estimating components of forest  
763 evapotranspiration: A footprint approach for scaling sap flux measurements. *Agric.*  
764 *For. Meteorol.* 248, 1719–1732.

765 Oren, R., Phillips, N., Katul, G., Ewers, B.E., Pataki, D.E., 1998. Scaling xylem sap flux  
766 and soil water balance and calculating variance: a method for partitioning water flux  
767 in forests. *Ann. Sci. For.* 55, 191–216.

768 Oren, R., Sperry, J.S., Katul, G.G., Pataki, D.E., Ewers, B.E., Phillips, N., Schäfer, K.V.R.,  
769 1999. Survey and synthesis of intra- and interspecific variation in stomatal sensitivity  
770 to vapour pressure deficit. *Plant Cell Environ.* 22, 1515–1526.

771 Peck, R., Devore, J.L., 2005. *Statistics: the Exploration and Analysis of Data*, Second  
772 Edition. Brooks/Cole, Boston, Massachusetts.

773 Phillips, N., Oren, R., 1998. A comparison of daily representations of canopy conductance  
774 based on two conditional time averaging methods and the dependence of daily  
775 conductance on environmental factors. *Ann. Sci. For.* 55, 217–235.

776 Running, S.W., Nemani, R.R. and Hungerford, R.D., 1987. Extrapolation of synoptic  
777 meteorological data in mountainous terrain, and its use for simulating forest  
778 evapotranspiration. *Can. J. For. Res.* 17, 472–483.

779 Scott, D.F., Lesch, W., 1997. Streamflow responses to afforestation with *Eucalyptus*

780 *grandis* and *Pinus petula* and to felling in the Mokobulaan experimental catchments,  
781 South Africa. J. Hydrol. 199, 360–377.

782 Shinohara, Y., Komatsu, H., Otsuki, K., 2007. A method for estimating global solar  
783 radiation from daily maximum and minimum temperatures: Its applicability to Japan.  
784 J. Jpn. Soc. Hydrol. Water Resour. 20, 462–469.

785 Shinohara, Y., Tsuruta, K., Ogura, A., Noto, F., Komatsu, H., Otsuki, K., Maruyama, T.,  
786 2013a. Azimuthal and radial variations in sap flux density and effects on stand-scale  
787 transpiration estimates in a Japanese cedar forest. Tree Physiol. 33, 550–558.

788 Shinohara, Y., Tsuruta, K., Kume, T., Otsuki, K., 2013b. An overview of stand-scale  
789 transpiration measurements using the sap flow technique for evaluating the effects of  
790 forest management practices. J. Jpn. For. Soc. 95, 321–331.

791 Stewart, J.B., Thom, A.S., 1973. Energy budgets in pine forest. Quart. J. Roy. Met. Soc.  
792 99, 154–170.

793 Sun, X., Onda, Y., Kato, H., Otsuki, K., Gomi, T., 2014. Partitioning of the total  
794 evapotranspiration in a Japanese cypress plantation during the growing season.  
795 Ecohydrol. 7, 1042–1053.

796 Suzuki, M., 1980. Evapotranspiration from a small catchment in hilly mountains (I)  
797 Seasonal variations in evapotranspiration, rainfall interception and transpiration. J. Jpn.  
798 For. Soc. 62, 46–53.

799 Tanaka, K., Tanaka, H., Nakamura, A., Ohte, N., Kobashi, S., 1996. Conductance at a

800 community level and characteristics of CO<sub>2</sub> exchange in hinoki (*Chamaecyparis*  
801 *obtusa*) stand. J. Jpn. For. Soc. 78, 266–272.

802 Tanaka, K., Kosugi, Y., Nakamura, A., 2002. Impact of leaf physiological characteristics  
803 on seasonal variation in CO<sub>2</sub>, latent and sensible heat exchanges over a tree plantation.  
804 Agric. For. Meteorol. 114, 103–122.

805 Tanaka, N., Kuraji, K., Shiraki, K., Suzuki, Y., Suzuki, M., Ohta, T., Suzuki, M., 2005.  
806 Throughfall, stemflow and rainfall interception at mature *Cryptomeria japonica* and  
807 *Chamaecyparis obtusa* stands in Fukuroyamasawa watershed. Bull. Tokyo Univ.  
808 Forest 113, 197–240.

809 The University of Tokyo Forests, 2014. Meteorological data. [http://www.uf.a.u-](http://www.uf.a.u-tokyo.ac.jp/eri/public.html)  
810 [tokyo.ac.jp/eri/public.html](http://www.uf.a.u-tokyo.ac.jp/eri/public.html).

811 Thompson, B., 1996. AERA editorial policies regarding statistical significance testing:  
812 three suggested reforms. Educational Res. 25, 26–30.

813 Thompson, B., 1998. Statistical significance and effect size reporting: Portrait of a  
814 possible future. Res. Sch. 5, 33–38.

815 Tsuruta, K., Kume, T., Komatsu, H., Higashi, N., Kumagai, T., Otsuki, K., 2008.  
816 Relationship between tree height and transpiration for individual Japanese Cypress  
817 (*Chamaecyparis obtusa*). J. Jpn. Soc. Hydrol. Water Resour. 21, 414–422.

818 Tsuruta, K., Komatsu, H., Shinohara, Y., Kume, T., Ichihashi, R., Otsuki, K., 2011.  
819 Allometric equations between stem diameter and sapwood area of Japanese cedar and

820 Japanese cypress for stand transpiration estimates using sap flow measurement. J. Jpn.  
821 Soc. Hydrol. Water Resour. 24, 261–270.

822 Tsuruta, K., Nogata, M., Shinohara, Y., Komatsu, H., Otsuki, K., 2014. The correction  
823 coefficient for leaf area index measurement based on the optical method in a Japanese  
824 cedar (*Cryptomeria japonica*) forest. Bull. Kyushu Univ. For. Accepted.

825 Tsuruta, K., Komatsu, H., Kume, T., Shinohara, Y., Otsuki, K., Canopy transpiration in  
826 two Japanese cypress forests with contrasting structures. Submitted to J. For. Res.

827 Xiang Y, Tateishi M, Saito T, Otsuki K, Kasahara T., Changes in canopy transpiration of  
828 Japanese cypress and Japanese cedar plantations due to selective thinning. Submitted  
829 to Hydrol. Process.

830 Yamanoi, K., Ohtani, Y., 1992. Eddy correlation measurements of energy budget and  
831 characteristics of evapotranspiration above a hinoki stand. J. Jpn. For. Soc. 74, 221–  
832 228.

833 Zwieniecki, M.A., Holbrook, N.M., 1998. Diurnal variation in xylem hydraulic  
834 conductivity in white ash (*Fraxinus americana* L.), red maple (*Acer rubrum* L.) and  
835 red spruce (*Picea rubens* Sarg.). Plant, Cell Environ. 21, 1173–1180.

836 Figure captions

837 Figure 1. Relationships (a) between vapor pressure deficit ( $D$ ) and canopy conductance  
838 ( $G_c$ ), (b) between solar radiation ( $R$ ) and  $G_c$  divided by  $G_{cref} f(D)$ , and (c) between  
839 temperature ( $T$ ) and  $G_c$  divided by  $G_{cref} f(D)g(R)$  for the OL site. Solid lines in Figures 1a,  
840 1b, and 1c indicate  $f(D)$ ,  $g(R)$ , and  $h(T)$  for OL, respectively.  $G_{cref}$  is the reference value  
841 of canopy conductance.  $f(D)$ ,  $g(R)$ , and  $h(T)$  are functions expressing the responses of  $G_c$   
842 to  $D$ ,  $R$ , and  $T$ .

843

844 Figure 2. Functions expressing the responses of canopy conductance to (a) vapor pressure  
845 deficit ( $f(D)$ ), (b) solar radiation ( $g(R)$ ), and (c) temperature ( $h(T)$ ) for each site.

846

847 Figure 3. Relationships of the mean transpiration ( $E$ ) for days with no rain and  
848 temperature being no less than 15 °C (i.e., corresponding to a growing season) calculated  
849 using (a) P1G, (b) P2G, and (c) P3G with the mean observed  $E$ . Here, P1G, P2G, and  
850 P3G respectively use the mean values of  $G_{cref}$ ,  $\beta$ , and  $\delta$  among the sites,  $G_{cref}$  determined  
851 for each site and the mean values of  $\beta$  and  $\delta$  among the sites, and  $G_{cref}$ ,  $\beta$ , and  $\delta$  determined  
852 for each site. The solid line indicates the 1:1 relationship. Dotted lines indicate conditions  
853 that errors in  $E$  estimates equal potential errors in observed  $E$ . Error bars indicate standard  
854 deviations.

855

856 Figure 4. Relationships of the mean transpiration ( $E$ ) for days with no rain calculated  
857 using (a) P1W, (b) P2W, and (c) P3W with the mean observed  $E$  for sites having data  
858 recorded in winter as well as those recorded in a growing season. Here, P1W, P2W, and  
859 P3W respectively use the mean values of  $G_{cref}$ ,  $\beta$ ,  $\delta$ ,  $\varepsilon$ , and  $\zeta$  among the sites,  $G_{cref}$   
860 determined for each site and the mean values of  $\beta$ ,  $\delta$ ,  $\varepsilon$ , and  $\zeta$  among the sites, and  $G_{cref}$ ,  
861  $\beta$ ,  $\delta$ ,  $\varepsilon$ , and  $\zeta$  determined for each site. The solid line indicates the 1:1 relationship. Dotted  
862 lines indicate conditions that errors in  $E$  estimates equal potential errors in observed  $E$ .  
863 Error bars indicate standard deviations.

864

865 Figure 5. Time series of daily transpiration ( $E$ ) calculated using P1W, P2W, and P3W and  
866 observed  $E$  for OU. Lines for P2W and P3W overlap each other.  $E$  observed on rainy days  
867 is not plotted in this figure.

868

869 Figure 6. Relationship between the sapwood area at a stand scale ( $A$ ) and the reference  
870 value of canopy conductance ( $G_{cref}$ ). The regression line for the relationship between  $A$   
871 and  $G_{cref}$ , determined using the least-squares method, is written as  $y = 0.157 x$ .

872

873 Figure 7. Normal probability plot for the difference between estimated and observed  
874 reference values of canopy conductance ( $G_{cref}$ ). The solid line is the regression line,  
875 determined using the least-squares method, for all data except those for SK and IK.

876

877 Figure 8. Comparison between estimated and observed sapwood areas on a stand scale

878 (A). The solid line indicates the 1:1 relationship.

879

880 Figure 9. Time series of daily transpiration ( $E$ ) calculated using P2W by omitting

881 functions expressing the responses of  $G_c$  to (a) vapor pressure deficit ( $f(D)$ ), (b) solar

882 radiation ( $g(R)$ ), and (c) temperature ( $h(T)$ ).

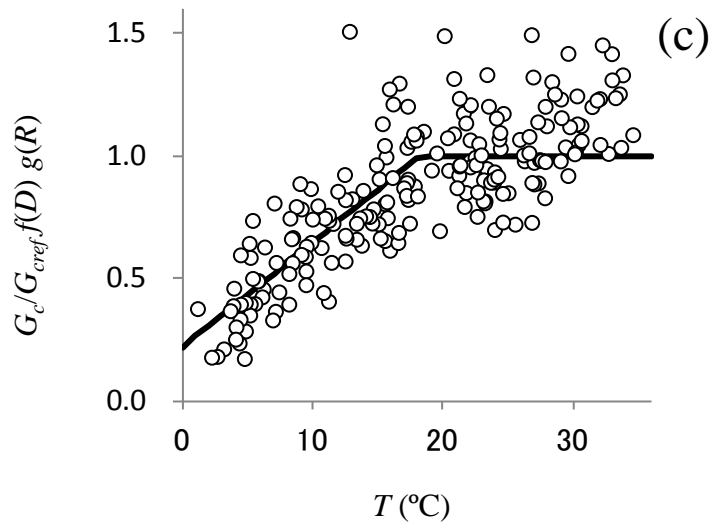
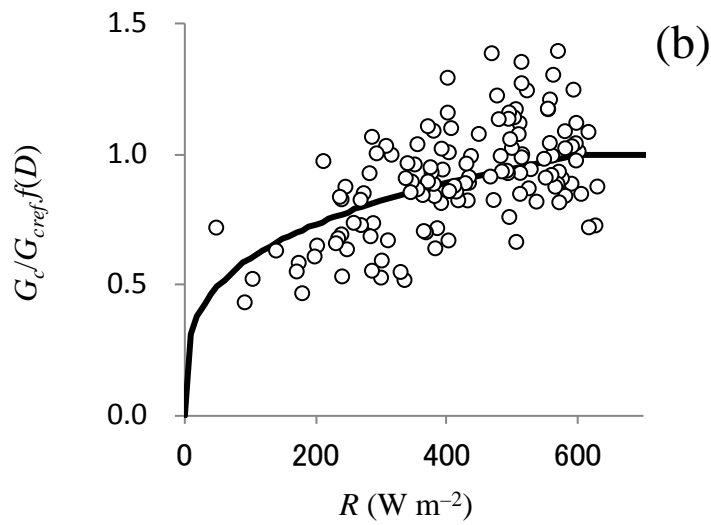
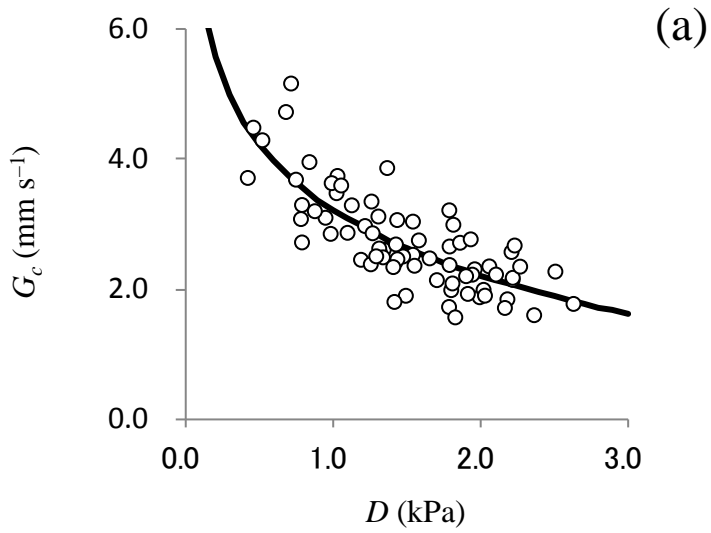


Figure 1



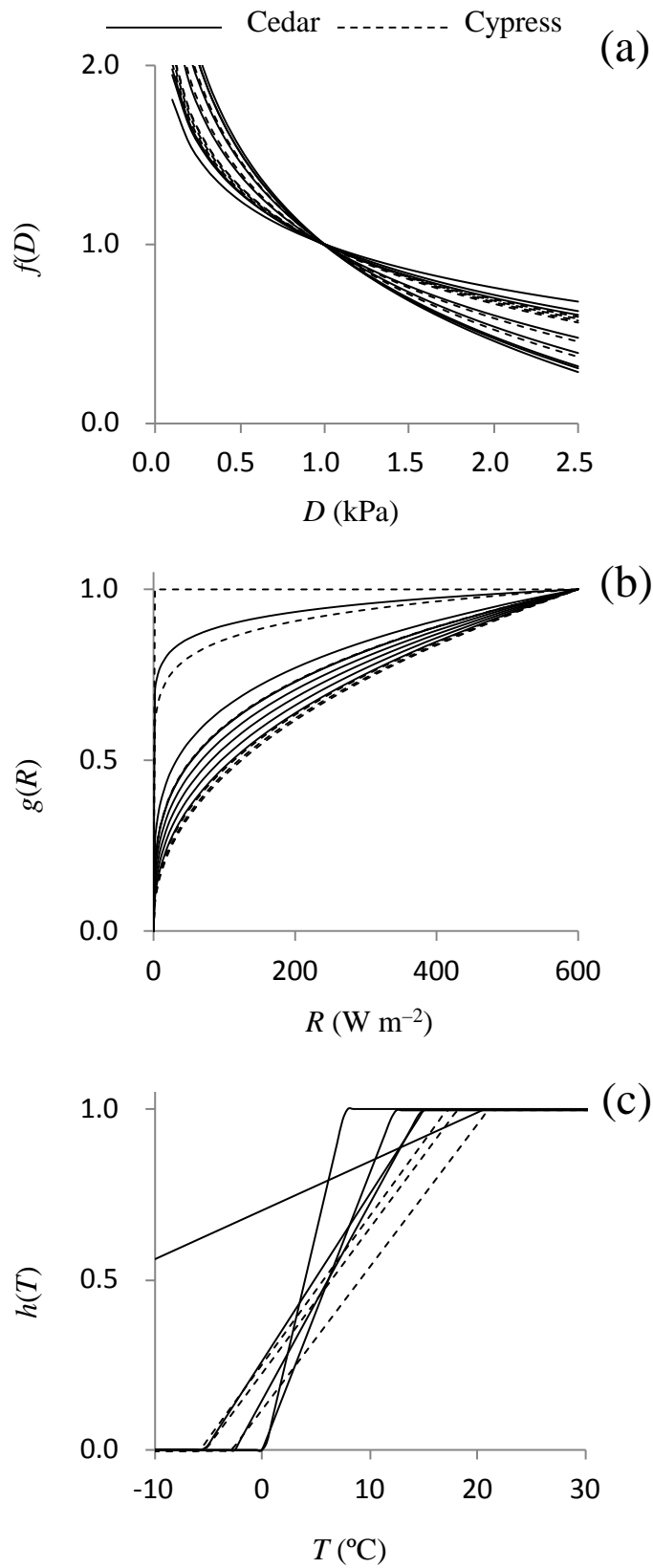


Figure 2

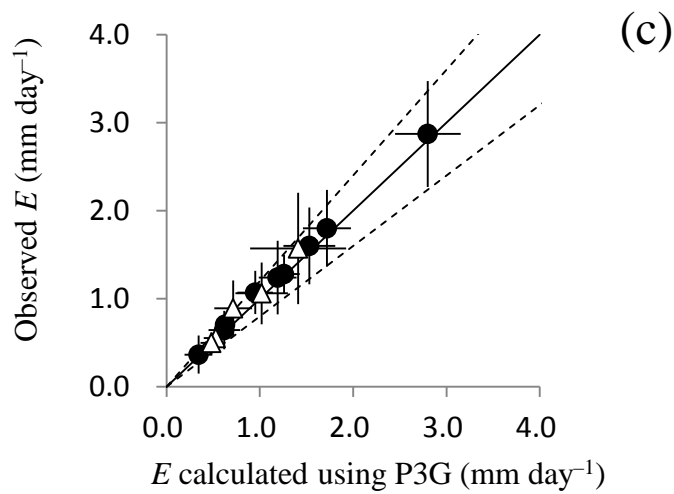
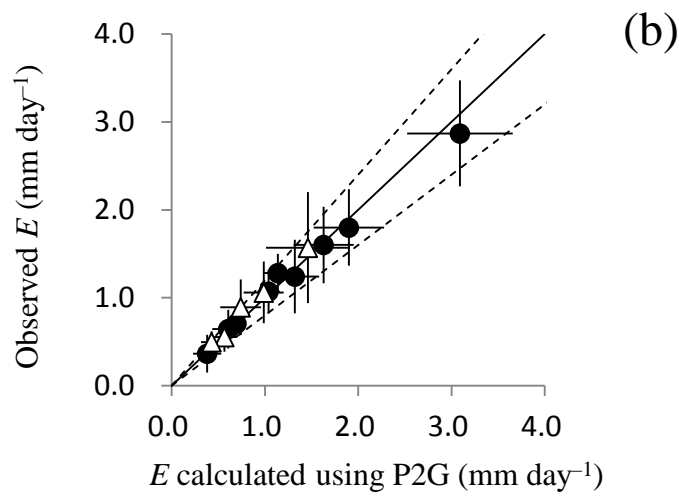
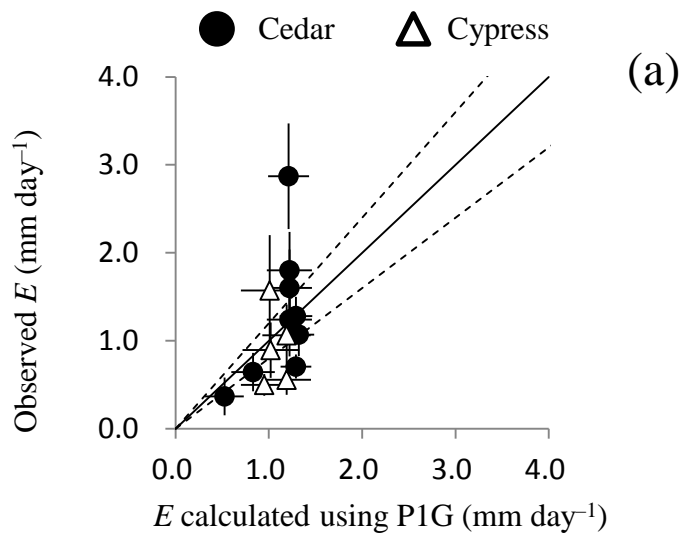


Figure 3

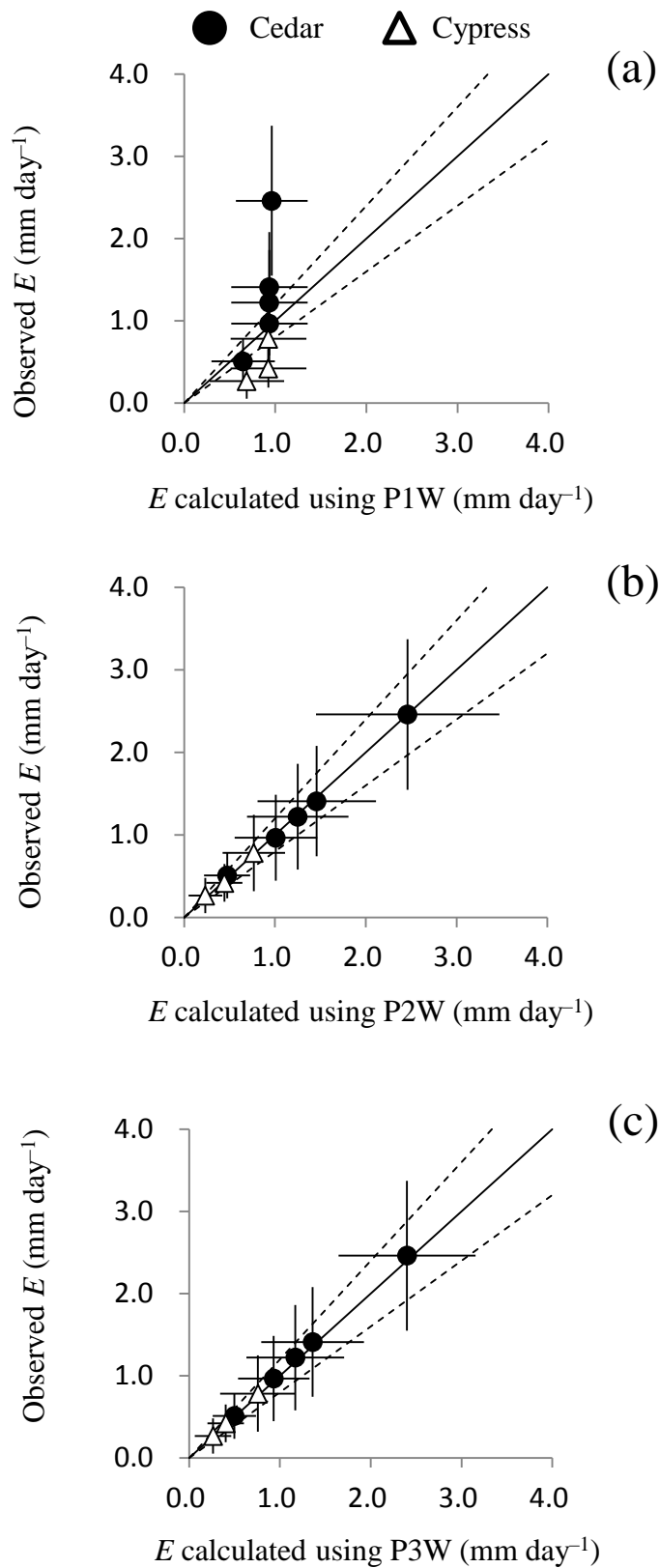


Figure 4

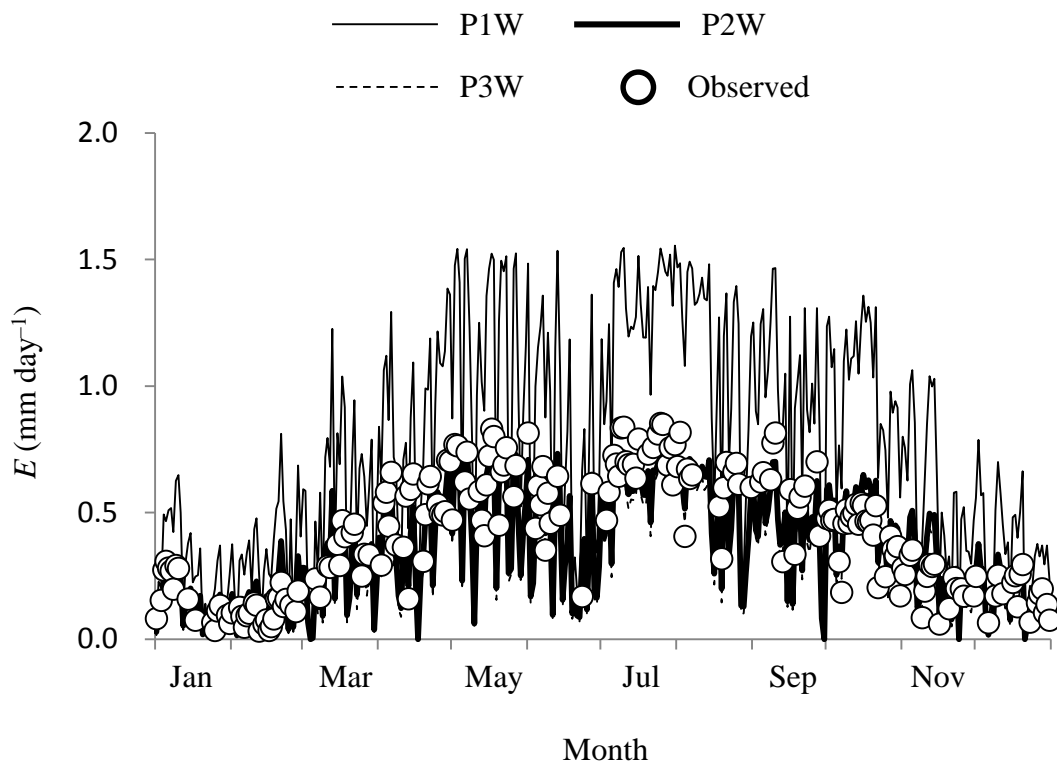


Figure 5

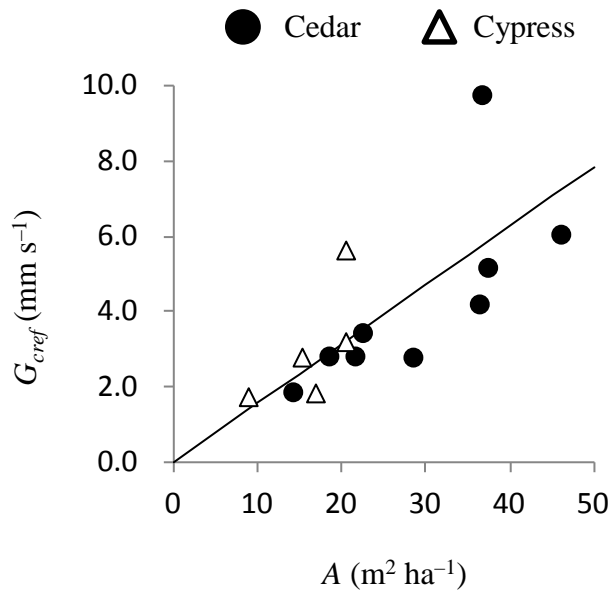


Figure 6

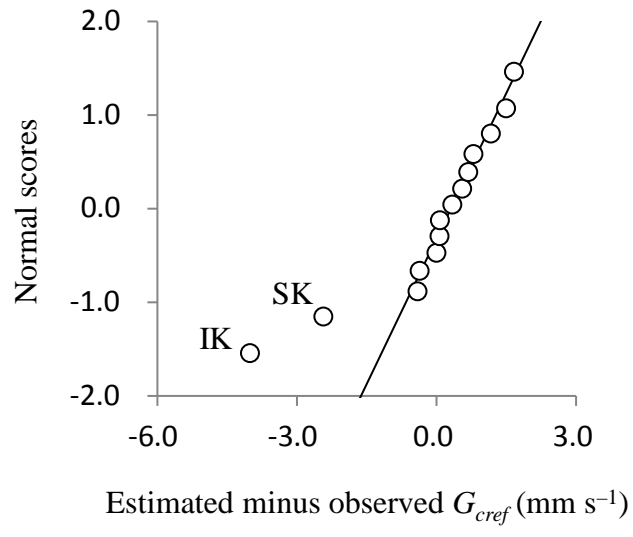


Figure 7

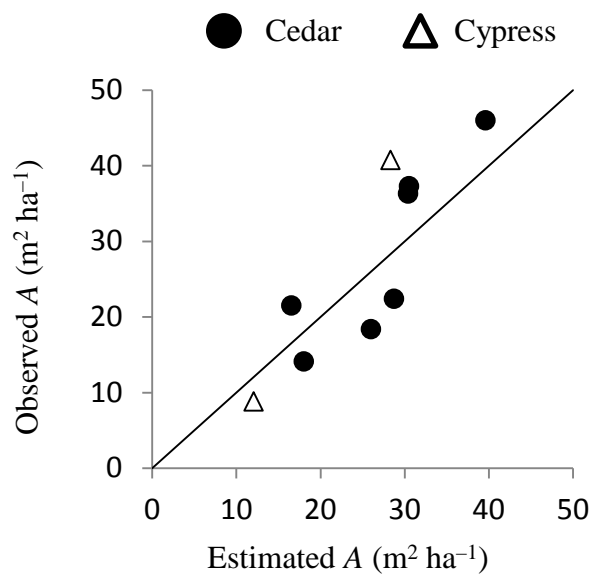


Figure 8

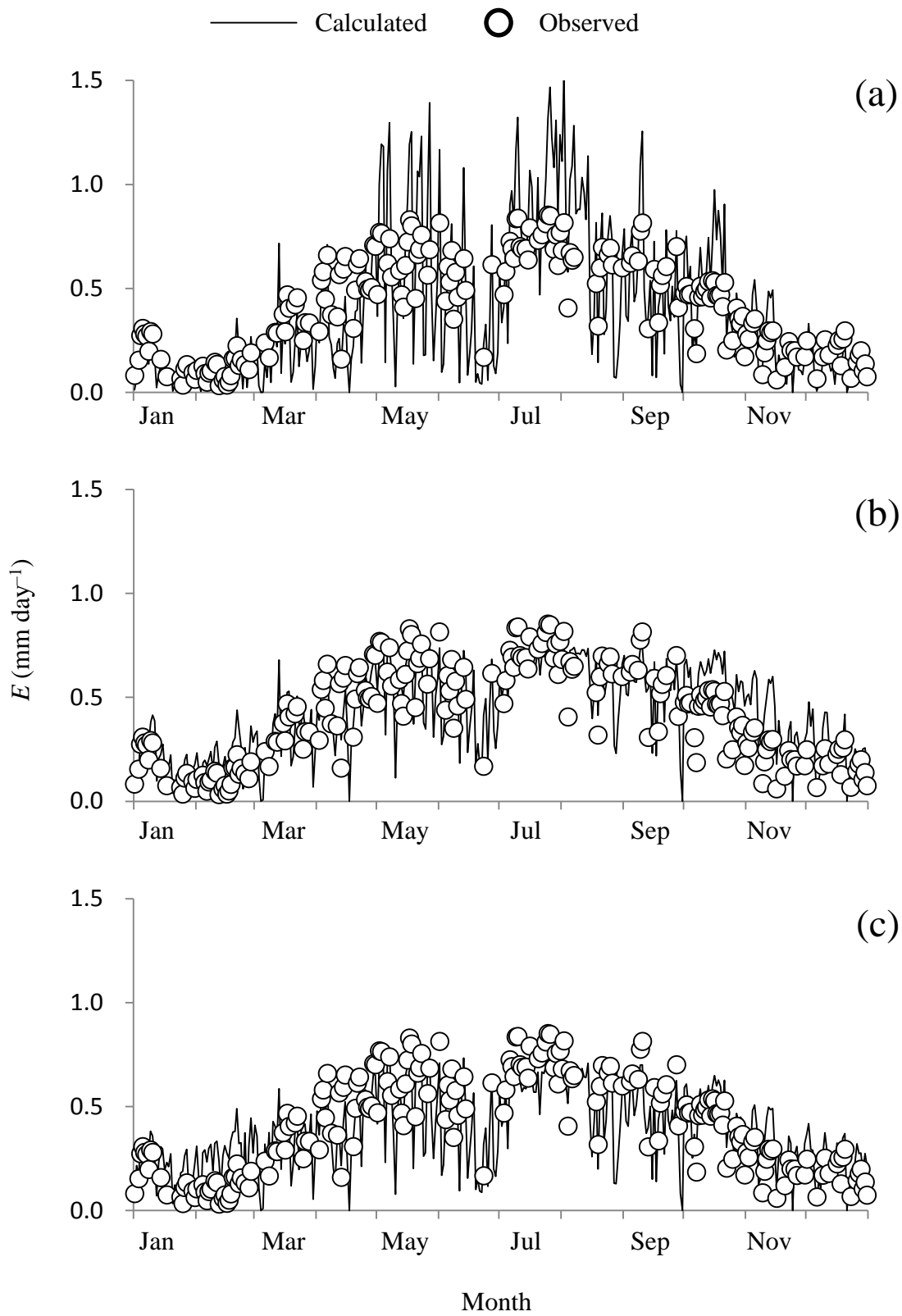


Figure 9



Table 1. Location, meteorology (the mean annual rainfall  $P$  and temperature  $T$ ), structure (stem density  $N$ , the mean diameter at breast height  $d_m$ , leaf area index  $L$ , and sapwood area  $A$ ), and description of sap-flux measurements for the plantation sites

Site	Location	$P$ (mm)	$T$ (°C)	Age (yr)	$N$ (stems ha <sup>-1</sup> )	$d_m$ (cm)	$L$ (m <sup>2</sup> m <sup>-2</sup> )* <sup>2</sup>	$A$ (m <sup>2</sup> ha <sup>-1</sup> )	Plot area (m <sup>2</sup> )	Number of the trees in the plot	Period	Reference
<i>Cedar</i>												
IK	36°N, 137°E	2814	12.7	55	600	48.4	3.2	36.6	300	18 (9) <sup>*3</sup>	May 15, 2010–May 24, 2011	Shinohara et al. (2013a)
YB	34°N, 131°E	1790	17.2	39	1100	28.9	4.7	22.4	100	11 (11)	Aug 1–Sept 31, 2010	Komatsu et al. (2013)
YA	34°N, 131°E	1790	17.2	40	600	31.6	2.3	14.1	100	6 (6)	Aug 1–Sept 31, 2011	Komatsu et al. (2013)
IS	34°N, 131°E	1807	15.9	43	658	28.2	0.8	21.5	213	14 (11)	May 22, 2012–Feb 28, 2013	Xiang et al. (submitted)
IR	34°N, 131°E	1790	17.2	60	1400	30.3	3.3	28.4	200	28 (14)	July 1–Aug 31, 2010	Ichihashi et al. (in press)
KL	33°N, 131°E	2150	15.0	50	904	40.3	5.7	46.0	321	29 (15)	Mar 3, 2007–July 3, 2008	Kumagai et al. (2007)
KU	33°N, 131°E	2150	15.0	50	1575	23.8	5.4	36.3	318	50 (23)	Mar 3, 2007–July 3, 2008	Kumagai et al. (2007)
KS	33°N, 131°E	2150	15.0	50	1330	26.6	5.9	37.3	203	27 (19)	Mar 3, 2007–July 3, 2008	Kumagai et al. (2014)
XT	24°N, 121°E	2635	17.0	60	625	39.0	2.6	18.4	400	25 (15)	Apr 14, 2012–Mar 19, 2013	Laplace (2013)
<i>Cypress</i>												
IH	34°N, 131°E	1807	15.9	43	863	20.2	0.8	8.8	197	17 (17)	May 22, 2012–Feb 28, 2013	Xiang et al. (submitted)
OL	34°N, 131°E	1790	17.2	49	1450	21.0	3.2	20.4	400	58 (14)	Jan 1–Dec 31, 2008	Kume et al. (2010)
OU	34°N, 131°E	1790	17.2	49	1700	14.9		16.8	100	58 (17)	Jan 1–Dec 31, 2008	Kume et al. (submitted)
SK	34°N, 131°E	1790	17.2	19	2100	13.5	4.8	20.4	100	21 (10)	Apr 1–Aug 15, 2009	Tsuruta et al. (submitted)
HW	34°N, 131°E	1790	17.2	99	350	44.6	3.1	15.2	200	7 (7)	Apr 1–Aug 31, 2009	Tsuruta et al. (submitted)

\*1 The original names of the sites are given as follows. IK: Ishikawa-ken Forest Experimental Station, YB: Yamanokami site (before thinning), YA: Yamanokami site (after thinning), IS: Yayama Experimental Catchment (cedar) in Iizuka, IR: Ichirinpan Plot in the Kasuya Research Forest, KU: UP of Kahoku Experimental Watershed, KL: LP of Kahoku Experimental Watershed, KS: SP of Kahoku Experimental Watershed, XT: Xitou Experimental Forest, IH: Yayama Experimental Catchment (cypress) in Iizuka, OL: Riparian Plot of Ochozu Experimental Watershed, OU: Ridge Plot of Ochozu Experimental Watershed, SK: Sakuta Plot in Kasuya Research Forest, HW: Hiawada Plot in Kasuya Research Forest

\*2  $L$  for all sites except OL and IK was measured using a plant-canopy analyzer (LAI-2000, Li-Cor Inc., Lincoln, Nebraska, USA).  $L$  for OL and IK was measured using a digital non-spherical color photograph and Gap Light Analyzer software (Franzer et al., 1999).

\*3 Numerals in the parentheses indicate the number of trees in which sensors were installed.

Table 2. Parameter values optimized for each site .

Site	$G_{cref}$ (mm s <sup>-1</sup> )	$\beta$ in $f(D)$	$R^2$	$\delta$ in $g(R)$	$R^2$	$\varepsilon$ (°C) in $h(T)$	$\zeta$ (°C) in $h(T)$	$R^2$
<i>Cedar</i>								
IK	9.77	0.750	0.782	0.287	0.389	7.75	0.313	0.469
YB	3.46	0.441	0.493	0.0893 <sup>*1</sup>	0.00793			
YA	1.89	0.427	0.365	0.0625 <sup>*1</sup>	0.00247			
IS	2.84	0.569	0.580	0.238	0.339	20.7	-48.8	0.164
IR	2.81	0.351	0.214	0.288	0.219			
KL	6.07	0.783	0.605	0.347	0.316	12.3	0.065	0.587
KU	4.22	0.749	0.438	0.410	0.240	15.1	-5.22	0.343
KS	5.19	0.667	0.628	0.378	0.392	14.8	-2.49	0.544
XT	2.84	0.412	0.213	0.308	0.310			
<i>Cypress</i>								
IH	1.76	0.472	0.622	0.000 <sup>*1</sup>	-0.0329	21.0	-2.84	0.740
OL	3.22	0.453	0.628	0.285	0.330	18.2	-5.19	0.636
OU	1.86	0.591	0.738	0.417	0.561	17.2	-5.78	0.584
SK	5.65	0.468	0.412	0.432	0.252			
HW	2.81	0.688	0.436	0.441	0.270			
Mean	3.89	0.556		0.285		15.9	-8.74	
Standard deviation	2.19	0.146		0.142		4.43	16.4	

<sup>\*2</sup> A small  $\delta$  value does not suggest that there was no effect of solar radiation on transpiration, but suggests that the effect was not detectable by an analysis on a daily time scale.

Table 3. Slope and coefficient of determination ( $R^2$ ) for the relationship between calculated and observed transpiration.

Site	P1W		P2W		P3W	
	Slope <sup>*1</sup>	$R^2$	Slope	$R^2$ <sup>*2</sup>	Slope	$R^2$
<i>Cedar</i>						
IK	2.43	0.329 <sup>*3</sup>	0.946	0.329	1.02	0.576
IS	0.776	0.867	1.06	0.867	1.03	0.874
KL	1.50	0.845	0.964	0.845	1.04	0.818
KU	1.05	0.757	0.970	0.757	1.06	0.726
KS	1.32	0.848	0.988	0.848	1.05	0.845
<i>Cypress</i>						
IH	0.510	0.927	1.13	0.927	1.02	0.937
OL	0.879	0.843	1.06	0.843	1.04	0.883
OU	0.466	0.891	0.974	0.891	1.05	0.911

<sup>\*1</sup> The intercept of the regression equation was assumed to be zero.

<sup>\*2</sup> Determination coefficients for P2W are identical to those for P1W, because the responses of canopy conductance to meteorological factors for P2W are same as those for P1W.

<sup>\*3</sup> Low determination coefficients for IK were primarily caused by the small number of data with low  $E$  due to rejection of data recorded on rainy days. When including data recorded on rainy days in the analysis, the determination coefficients were 0.829, 0.829, and 0.858 for P1W, P2W, and P3W, respectively.